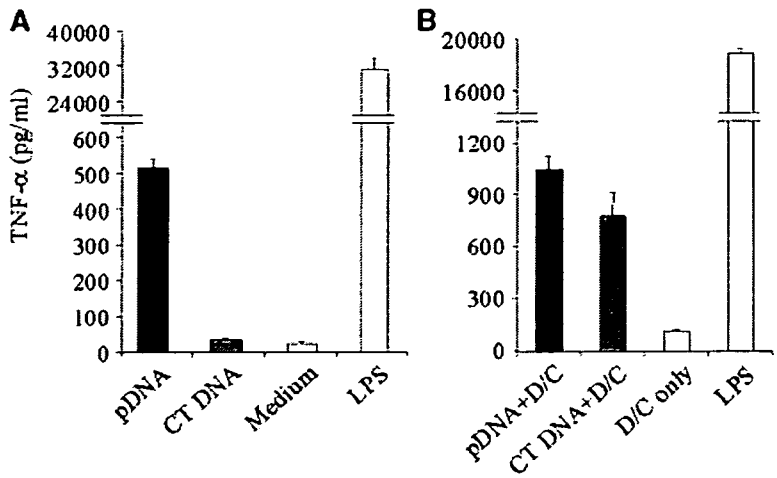

Figure 5. TNF-α secretion by DNA from RAW264.7 cells. Cells were incubated with naked DNA (5 μg/mL) (A) or DNA/cationic liposome complex (5:35.09 μg/mL) (B). After a 2-h incubation, the complexes were removed and fresh growth medium was added to the cells. The supernatants were collected 8 h after addition of naked DNA or DNA complex. LPS was used at a concentration of 1 ng/mL. The concentration of TNF-α secreted from RAW264.7 cells was quantified by ELISA. Each result represents the mean and standard deviation of triplicate values.

DISCUSSION

Many *in vivo* studies using mice have shown that naked pDNA and pDNA/cationic liposome complexes stimulate significant cytokine production.[9,28–30] Although there is a growing body of information about macrophage activation by CpG DNA, most studies have been performed using murine macrophage cell lines, such as RAW264.7. Few studies have been reported using primary cultured macrophages freshly isolated from animals, which would be a better model than immortalized cell lines.

In the present study, we used primary cultured cells, including hepatic NPCs, splenic macrophages, mesangial cells and peritoneal macrophages. Liver and spleen play a central role in the removal of foreign particles from the circulation mainly via Kupffer cells and splenic macrophages.[31,32] In the kidney, mesangial cells, which play a central role in the physiology and pathophysiology of the glomerulus, are also reported to exhibit phagocytic or endocytic activity.[33] CpG DNA requires endocytosis for specific recognition by intracellular TLR9 for immunoactivation.[4,14,34,35] Therefore, we first quantitatively evaluated the TLR9 expression in the mRNA and protein levels (Fig. 1). We confirmed that primary cultured cells, peritoneal macrophages, splenic macrophages and hepatic NPCs, expressed TLR9. No TLR9 mRNA was detected in mesangial cells, as previously reported.[36,37] It has been reported that the expression level of TLR was altered not only when macrophages were exposed to inflammatory cytokines but also when cells were isolated from inflammatory disease patients,[38,39] suggesting that the TLR9 expression is regulated by various factors, including cytokines and pathogens. Therefore, the level of TLR9 expression in various types of macrophages might reflect the immunological milieu of tissues where the cells are isolated.

Next, we examined the cellular activation of primary cultured cells by the ligand of TLR9, naked CpG DNA at initial concentrations of 10 and/or 100 μg/mL. Nichols et al.[40] reported that pDNA remains intact for several hours after intramuscular injection in mice. In addition, naked pDNA can induce inflammatory cytokines after intravenous injection at a high dose of 250 μg/mouse.[41] Under these conditions, the initial plasma concentration of pDNA can be as high as 200 μg/mL so that the concentration could be over 10 μg/mL, the concentration used in the present study, for some time. Selective uptake of DNA by macrophages would take place after its systemic administration, which would also increase the local concentration of DNA around the cells. The dose of 250 μg pDNA seems to be high, but pDNA up to a few hundred micrograms

have been used for gene transfer to mice. In addition, the diffusion of pDNA within the tissues injected is severely limited because of its macromolecular nature, and the local concentration can be higher at the injection sites.

Binding of TLRs to their ligands leads to cellular activation and inflammatory cytokine production, and this responsiveness corresponded to the level of TLRs expression.[42] Therefore, it was expected that TNF-α would be produced in parallel with the level of TLR9 expressed in the cells. Predictably, splenic macrophages and hepatic NPCs secreted TNF-α by naked DNA in a CpG motif-dependent manner (Figs. 2 and 3). When splenic macrophages and hepatic Kupffer cells were functionally depleted by preloading clodronate liposomes into mice, TNF-α levels in spleen and liver were significantly reduced after intravenous injection of naked DNA.[41] The results in the present study clearly indicate the involvement of splenic macrophages and hepatic NPCs in the inflammatory responses to pDNA *in vivo*. In addition to Kupffer cells, liver sinusoidal endothelial cells (LSECs), which are another major component of hepatic NPCs, have been reported to express TLR9 mRNA and produce IL-1β and IL-6 following the addition of CpG-oligonucleotides.[43] Not only Kupffer cells but also LSECs play an important role in the immune response to CpG DNA because both types of cells are major contributors to the hepatic uptake of pDNA after intravenous injection.[26]

Some differences have been noticed in the CpG DNA-mediated cellular activation among the several types of macrophages cell lines.[44] Of various types of cell lines, we selected RAW264.7 cells as a reference type of macrophagelike cells in the present study, because RAW264.7 cells (i) release cytokines upon addition of CpG DNA and (ii) have been extensively used in previous studies. To our surprise, RAW264.7 cells expressed a lower level of TLR9 than the primary macrophages even although they were activated to produce a large amount of TNF-α upon addition of plasmid DNA. A high responsiveness of RAW264.7 cells was also noticed when added with LPS, the TLR4 ligand, compared with primary macrophages. These findings suggest that the cytokine production of RAW264.7 cells is efficient compared with that of primary macrophages. Differences in the expression of molecules involved in the cytokine production except for the TLRs may explain such differences in TNF-α production observed between RAW264.7 cells and primary macrophages. These results also indicate the importance of the use of primary macrophages, not macrophage cell lines, for estimating the events occurring in the body after administration of DNAs, such as pDNA.

A positive relation was clearly observed between the level of TLR9 expression and the level of TNF-α production when primary cultured macrophages were used. Despite of the expression of TLR9, resident peritoneal macrophages did not produce any TNF-α. Previous studies reported that thioglycollate-elicited, activated macrophages effectively induce inflammatory cytokines by CpG-ODN.[3,42] We also found that resident peritoneal macrophages release TNF-α by addition of CpG-ODN 1668, a highly potent stimulator of murine TLR9.[14] These results suggest that nonactivated peritoneal macrophages have low responsiveness to naked pDNA compared with splenic macrophages and hepatic NPCs. In addition, it was also confirmed that the immunostimulatory activity of pDNA is very low compared with that of phosphorothioate-type CpG-ODN. Again, other factors than the TLR9 involved in the TLR9 pathway would also be responsible to the level of cytokine production in TLR9-positive cells.

In the case of cationic liposomes, only splenic macrophages were activated by pDNA/DOTMA/cholesterol liposome complexes in a CpG motif-dependent manner and other primary cultured cells were not activated at all. We and other groups have reported that DNA/cationic liposome complexes accumulate in the liver and spleen after intravenous administration and hepatic Kupffer cells and splenic macrophages are directly involved in the uptake of DNA/cationic liposome complexes and inflammatory cytokine production.[13,45–48] In this respect, the results obtained from the present *in vitro* study did not agree completely with those obtained from the *in vivo* studies. No significant TNF-α production was observed by stimulation with the DNA/cationic liposome complexes in the liver NPC in primary culture (Fig. 3). In the present study, the level of induced TNF-α in the NPC preparations was very low even after treatment with a high concentration of LPS (1 μg/mL). Previous studies have also reported a low responsiveness of mouse Kupffer cells in primary culture to LPS.[49,50] The preparations might have a very low responsiveness to the DNA complexes via TLR9.

In this study, pDNA/DOTMA/cholesterol liposome complexes did not induce TNF-α production in peritoneal macrophages in spite of having many

DOI 10.1002/jps

CpG motifs. On the other hand, we have already reported that TNF-α is produced from resident peritoneal macrophages by another DNA/cationic liposome, Lipofectamine plus reagent (LAplus), complex. Moreover, this cytokine production is independent of the presence of not only CpG motifs but also TLR9. The discrepancy between the present and previous studies is due to the difference in the composition of cationic liposomes; the type of lipid contained in cationic liposomes alters the cellular trafficking of the DNA complexed with the liposome.[51,52] We showed that splenic macrophages are activated to produce TNF-α by pDNA/DOTMA/cholesterol liposome complexes (Fig. 2B), but not by pDNA/LAplus complexes (data not shown). On the other hand, RAW264.7 cells produced TNF-α by both DNA/cationic liposome complexes independent of CpG motifs (Fig. 5B, Ref.[17]). Other groups have demonstrated that double-stranded DNA complexed with cationic liposomes could induce type I interferon independent of CpG motifs in mouse embryonic fibroblasts or HEK293 cells which did not express TLR9.[53,54] Most recently, Takaoka et al. reported a cytoplasmic DNA sensor DAI, which recognizes double-stranded DNA and activates innate immune responses independent of TLR9.[55] However, it remains to be determined whether DAI is ubiquitously expressed in various types of tissue macrophages. The results in the present study indicate that the immune responses induced by DNA/cationic liposome complexes are dependent on the cell types and/or lipid composition of the cationic liposomes. Further studies are required to clarify TLR9-independent immune responses to DNA complexes.

In conclusion, we have demonstrated that primary cultured splenic macrophages and hepatic NPCs are able to produce inflammatory cytokines by naked DNA in a CpG motif-dependent manner *in vitro*. Moreover, TNF-α production induced by DNA/cationic liposome complexes is partially independent of the CpG motifs and there are differences in inflammatory response between various primary cultured cells. These findings provide valuable information to increase our understanding of macrophage activation by pDNA *in vivo*.

ACKNOWLEDGMENTS

This work is partly supported both by 21st Century COE Program "Knowledge Information Infrastructure for Genome Science" and by a grant-in-aid for Scientific Research from the Ministry of Education, Culture, Sports, Sciences and Technology, Japan.

REFERENCES

1. Wolfgang WL, Han Y, Nicholas PR. 1999. DNA and RNA-based vaccines: Principles, progress and prospects. Vaccine 18:765–777.
2. Wagner H. 1999. Immunobiology of bacterial CpG-DNA. In: Wagner H, Compans RW, Copper M, Hogle JM, Ito Y, Koprowski H, Melchers F, Oldstone M, Olsnes S, Potter M, Saedler H, Vogt PK, editors. Current topics in microbiology and immunology. Vol. 247. Berlin: Germany, Springer.
3. Hemmi H, Takeuchi O, Kawai T, Kaisho T, Sato S, Sanjo H, Matsumoto M, Hoshino K, Wagner H, Takeda K, Akira S. 2000. A Toll-like receptor recognizes bacterial DNA. Nature 408:740–745.
4. Ahmad-Nejad P, Häcker H, Rutz M, Bauer S, Vabulas RM, Wagner H. 2002. Bacterial CpG-DNA and lipopolysaccharides activate Toll-like receptors at distinct cellular compartments. Eur J Immunol 32:1958–1968.
5. Qin L, Ding Y, Pahud DR, Chang E, Imperiale MJ, Bromberg JS. 1997. Promoter attenuation in gene therapy: Interferon-gamma and tumor necrosis factor-alpha inhibit transgene expression. Hum Gene Ther 8:2019–2029.
6. Ghazizadeh S, Carroll JM, Taichman LB. 1997. Repression of retrovirus-mediated transgene expression by interferons: Implications for gene therapy. J Virol 71:9163–9169.
7. Paillard F. 1999. CpG: The Double-Edged Sword. Hum Gene Ther 10:2089–2090.
8. Alton EWFW, Geddes DM, Gill DR, Higgins CF, Hyde SC, Innes JA, Porteous DJ. 1998. Towards gene therapy for cystic fibrosis: A clinical progress report. Gene Ther 5:291–292.
9. Freimark BD, Blezinger HP, Florack VJ, Nordstrom JL, Long SD, Deshpande DS, Nochumson S, Petrak KL. 1998. Cationic lipids enhance cytokine and cell influx levels in the lung following administration of plasmid: Cationic lipid complexes. J Immunol 160:4580–4586.
10. Yew NS, Zhao H, Wu IH, Song A, Tousignant JD, Przybylska M, Cheng SH. 2001. Reduced inflammatory response to plasmid DNA vectors by elimination and inhibition of immunostimulatory CpG motifs. Mol Ther 1:255–262.
11. Kawabata K, Takakura Y, Hashida M. 1995. The fate of plasmid DNA after intravenous injection in mice: Involvement of scavenger receptors in its hepatic uptake. Pharm Res 12:825–830.
12. Yoshida M, Mahato RI, Kawabata K, Takakura Y, Hashida M. 1996. Disposition characteristics of plasmid DNA in the single-pass rat liver perfusion system. Pharm Res 13:599–603.

13. Sakurai F, Terada F, Yasuda K, Yamashita F, Takakura Y, Hashida M. 2002. The role of tissue macrophages in the induction of proinflammatory cytokine production following intravenous injection of lipoplexes. Gene Ther 9:1120–1126.
14. Yasuda K, Kawano H, Yamane I, Ogawa Y, Yoshinaga T, Nishikawa M, Takakura Y. 2004. Restricted cytokine production from mouse peritoneal macrophages in culture in spite of extensive uptake of plasmid DNA. Immunology 111:282–290.
15. Takagi T, Hashiguchi M, Mahato RI, Tokuda H, Takakura Y, Hashida M. 1998. Involvement of specific mechanism in plasmid DNA uptake by mouse peritoneal macrophages. Biochem Biophys Res Commun 245:729–733.
16. Takakura Y, Takagi Y, Hashiguchi M, Nishikawa M, Yamashita F, Doi T, Imanishi T, Suzuki H, Kodama T, Hashida M. 1999. Characterization of plasmid DNA binding and uptake by peritoneal macrophages from class A scavenger receptor knockout mice. Pharm Res 16:503–508.
17. Yasuda K, Ogawa Y, Kishimoto M, Takagi T, Hashida M, Takakura Y. 2002. Plasmid DNA activates murine macrophages to induce inflammatory cytokines in a CpG motif-independent manner by complex formation with cationic liposomes. Biochem Biophys Res Commun 293:344–348.
18. Yasuda K Ogawa Y, Yamane I, Nishikawa M, Takakura Y. 2005. Macrophage activation by a DNA/cationic liposome complex requires endosomal acidification and TLR9-dependent and -independent pathways. J Leukoc Biol 77:71–79.
19. Yasuda K, Yu P, Kirschning CJ, Schlatter B, Schmitz F, Heit A, Bauer S, Hochrein H, Wagner H. 2005. Endosomal translocation of vertebrate DNA activates dendritic cells via TLR9-dependent and -independent pathways. J Immunol 174:6129–6136.
20. Nomura T, Yasuda K, Yamada T, Okamoto S, Mahato RI, Watanabe Y, Takakura Y, Hashida M. 1999. Gene expression and antitumor effects following direct interferon (IFN)-gamma gene transfer with naked plasmid DNA and DC-chol liposome complexes in mice. Gene Ther 6:121–129.
21. Klinman DM, Yi AK, Beaucage SL, Conover J, Krieg AM. 1996. CpG motifs present in bacterial DNA rapidly induce lymphocytes to secrete interleukin 6, interleukin 12, and interferon γ. Proc Natl Acad Sci 93:2879–2883.
22. Cotton M, Baker A, Saltik M, Wagner E, Buschle M. 1994. Gene expression and antitumor effects following direct interferon (IFN)-gamma gene transfer with naked plasmid DNA and DC-chol liposome complexes in mice. Gene Ther 1:239–246.
23. Hartmann G, Krieg AM. 1999. CpG DNA and LPS induce distinct patterns of activation in human monocytes. Gene Ther 6:893–903.
24. Templeton NS, Lasic DD, Frederik PM, Strey HH, Roberts DD, Pavlakis GN. 1997. Improved DNA: Liposome complexes for increased systemic delivery and gene expression. Nat Biotechnol 15:647–652.
25. Sakurai F, Nishioka T, Saito H, Baba T, Okuda A, Matsumoto O, Taga T, Yamashita F, Takakura Y, Hashida M. 2002. Interaction between DNA-cationic liposome complexes and erythrocytes is an important factor in systemic gene transfer via the intravenous route in mice: The role of the neutral helper lipid. Gene Ther 8:677–686.
26. Hisazumi J, Kobayashi N, Nishikawa M, Takakura Y. 2004. Significant role of liver sinusoidal endothelial cells in hepatic uptake and degradation of naked plasmid DNA after intravenous injection. Pham Res 21:1223–1228.
27. Mori T, Bartocci A, Satriano J, Zuckerman A, Stanley R, Santiago A, Schlondorff D. 1990. Mouse mesangial cells produce colony-stimulating factor-1 (CSF-1) and express the CSF-1 receptor. J Immunol 144:4697–4702.
28. Tan Y, Li S, Pitt BR, Huang L. 1999. The inhibitory role of CpG immunostimulatory motifs in cationic lipid vector-mediated transgene expression in vivo. Hum Gene Ther 10:2153–2161.
29. Macfarlane DE, Manzel L. 1999. Immunostimulatory CpG-oligodeoxynucleotides induce a factor that inhibits macrophage adhesion. J Lab Clin Med 134:501–509.
30. Rudginsky S, Siders W, Ingram L, Marshall J, Scheule R, Kaplan J. 2001. Antitumor activity of cationic lipid complexed with immunostimulatory DNA. Mol Ther 4:347–355.
31. Zhang Y, Chirmule N, Gao GP, Qian R, Croyle M, Joshi B, Tazelaar J, Wilson JM. 2001. Acute cytokine response to systemic adenoviral vectors in mice is mediated by dendritic cells and macrophages. Mol Ther 3:697–707.
32. Egmond M, Garderen E, Spriel AB, Damen CA, Amersfoort ES, Zandbergen G, Hattum J, Kuiper J, Winkel JG. 2000. FcαRI-positive liver Kupffer cells: Reappraisal of the function of immunoglobulin A in immunity. Nat Med 6:680–685.
33. Savill J, Smith J, Sarraf C, Ren Y, Abbott F, Rees A. 1992. Glomerular mesangial cells and inflammatory macrophages ingest neutrophils undergoing apoptosis. Kidney Int 42:924–936.
34. Manzel L, Macfarlane DE. 1999. Lack of immune stimulation by immobilized CpG-oligodeoxynucleotide. Antisense Nucleic Acid Drug Dev 9:459–464.
35. Häcker H, Mischak H, Miethke T, Liptay S, Schmid R, Sparwasser T, Heeg K, Lipford GB, Wagner H. 1998. CpG-DNA-specific activation of antigen-presenting cells requires stress kinase activity and is preceded by non-specific endocytosis and endosomal maturation. EMBO J 17:6230–6240.
36. Patole PS, Pawar RD, Lech M, Zecher D, Schmidt H, Segerer S, Ellwart A, Henger A, Kretzler M,

Anders HJ. 2006. Expression and regulation of Toll-like receptors in lupus-like immune complex glomerulophritis of MRL-Fas(lpr) mice. Nephrol Dial Transplant 21:3062–3073.
37. Anders HJ, Vielhauer V, Eis V, Linde Y, Kretzler M, Lema GP, Strutz F, Bauer S, Rutz M, Wagner H, Grone HJ, Schlondorff D. 2004. Activation of toll-like receptor-9 induces progression of renal disease in MRL-Fas(LPR) mice. FASEB J 18:534–536.
38. Baiyee EE, Flohe S, Lendemans S, Bauer S, Mueller N, Kreuzfelder E, Grosse-Wilde H. 2006. Expression and function of Toll-like receptor 9 severely injured patient prone to sepsis. Clin Exp Immunol 145:456–462.
39. Pedersen G, Andersen L, Matthiessen MW, Rask-Madsen J, Brynskov J. 2005. Expression of Toll-like receptor 9 and response to bacterial CpG oligodeoxynucleotides in human intestinal epithelium. Clin Exp Immunol 141:298–306.
40. Manam S, Ledwith BJ, Barnum AB, Troilo PJ, Pauley CJ, Harper LB, Griffiths TG II, Niu Z, Denisova L, Follmer TT, Pacchione SJ, Wang Z, Beare CM, Bagdon WJ, Nichols WW. 2000. Plasmid DNA vaccines: Tissue distribution and effects of DNA sequence, adjuvants and delivery method on integration into host DNA. Interviology 43:273–281.
41. Kako K, Nishikawa M, Yoshida H, Takakura Y. 2007. Effect of inflammatory response on in vivo transgene expression by plasmid-DNA in mice. J Pharm Sci, in press.
42. Renshaw M, Rockwell J, Engleman C, Gewirtz A, Katz J, Sambhara S. 2002. Impaired toll-like receptor expression and function in aging. J Immunol 169:4697–4701.
43. Montserrat MA, Jaione SS, Ingvild P, Ugo M, Bard S, Baldur S. 2006. Toll-like receptor 9 (TLR9) is present in murine liver sinusoidal endothelial cells (LSECs) and mediates the effect of CpG-oligonucleotides. J Hepatol 44:939–946.
44. Yamane I, Nishikawa M, Takakura Y. 2005. Cellular uptake and activation characteristics of naked plasmid DNA and its cationic liposome complex in human macrophages. Int J Pharm 305:145–153.
45. McLean JW, Fox EA, Baluk P, Bolton PB, Haskell A, Pearlman R, Thurston G, Umemoto EY, McDonald DM. 1997. Organ-specific endothelial cell uptake of cationic liposome-DNA complexes in mice. Am J Physiol 273:384–404.
46. Mahato RI, Kawabata K, Nomura T, Takakura Y, Hashida M. 1995. Physicochemical and pharmacokinetic characteristics of plasmid DNA/cationic liposome complexes. J Pharm Sci 84:1267–1271.
47. Osaka G, Carey K, Cuthbertson A, Godowski P, Patapoff T, Ryan A, Gadek T, Mordenti J. 1996. Pharmacokinetics, tissue distribution, and expression efficiency of plasmid [33P]DNA following intravenous administration of DNA/cationic lipid complexes in mice: Use of a novel radionuclide approach. J Pharm Sci 85:612–618.
48. Litzinger DC, Brown JM, Wala I, Kaufman SA, Van GY, Farrell CL, Collins D. 1996. Fate of cationic liposomes and their complex with oligonucleotide in vivo. Biochem Biophys Acta 1281:139–149.
49. Shih-Ching K, Choudhry MA, Matsutani T, Schwacha MG, Rue LW, Bland KI, Chaudry IH. 2004. Splenectomy differentially influences immune responses in various tissue compartments of the body. Cytokine 28:101–108.
50. Thobe BM, Frink M, Hildebrand F, Schwacha MG, Hubbard WJ, Choudhry MA, Chaudry IH. 2007. The role of MAPK in Kupffer cell toll-like receptor (TLR) 2-, TLR4-, and TLR9-mediated signaling following trauma-hemorrhage. J Cell Physiol 210:667–675.
51. Zuhorn IS, Hoekstra D. 2002. On the mechanism of cationic amphiphile-mediated transfection. To fuse or not to fuse: Is that the question? J Membr Biol 189:167–179.
52. Lee TWR, Matthews DA, Blair GE. 2005. Novel molecular approaches to cystic fibrosis gene therapy. Biochem J 387:1–15.
53. Ishii KJ, Coban C, Kato H, Takahashi K, Torii Y, Takeshita F, Ludwig H, Sutter G, Suzuki K, Hemmi H, Sato S, Yamamoto M, Uematsu S, Kawai T, Takeuchi O, Akira S. 2006. A Toll-like receptor–independent antiviral response induced by double-stranded B-form DNA. Nat Immunol 7:40–48.
54. Shirota H, Ishii KJ, Takakuwa H, Klinman DM. 2006. Contribution of interferon-beta to the immune activation induced by double-stranded DNA. Immunology 118:302–310.
55. Takaoka A, Wang Z, Choi MK, Yanai H, Negishi H, Ban T, Lu Y, Miyagishi M, Kodama T, Honda K, Ohba Y, Taniguchi T. 2007. DAI (DLM-1/ZBP1) is a cytosolic DNA sensor and an activator of innate immune response. Nature 448:501–505.

Gene Therapy (2008), 1–11

www.nature.com/gt

ORIGINAL ARTICLE

Inhibition of tumor cell growth in the liver by RNA interference-mediated suppression of HIF-1α expression in tumor cells and hepatocytes

Y Takahashi, M Nishikawa and Y Takakura
Department of Biopharmaceutics and Drug Metabolism, Graduate School of Pharmaceutical Sciences, Kyoto University, Kyoto, Japan

Hypoxia-inducible factor-1 (HIF-1) is a ubiquitously expressed oxygen-regulated transcription factor composed of α and β subunits. HIF-1 activates transcription of various genes including those involved in metastatic tumor growth. In the present study, HIF-1α expression in tumor-bearing mouse liver was examined after inoculation of tumor cells into portal vein. We found that tumor-bearing liver showed greatly increased HIF-1α expression. Plasmid DNA (pDNA) expressing short hairpin RNA targeting HIF-1α (pshHIF-1α) was effective in suppressing protein expression of HIF-1α in vitro. Intravenous injection of pshHIF-1α by hydrodynamics-based procedure reduced the HIF-1α protein expression in both normal and tumor cells and tumor cell number in the liver. Pre-injection of pshHIF-1α to mice, by which pDNA was delivered only to liver cells, not to tumor cells, was also effective in reducing the number of tumor cells inoculated 3 days after pDNA injection. These findings indicate that HIF-1α expression is increased in normal liver cells as well as tumor cells, and HIF-1α expression plays an important role in tumor progression. Use of the RNA interference (RNAi) of HIF-1 is an effective strategy for inhibiting tumor cell growth, and both tumor and normal cells can be the target for RNAi-based anticancer treatment.
Gene Therapy advance online publication, 14 February 2008; doi:10.1038/sj.gt.3303103

Keywords: *RNAi; HIF-1α; gene delivery; hydrodynamics-based procedure; hepatic metastasis*

Introduction

Metastasis, which is the transfer of cancer cells from one organ to other organs, is the most distinctive feature of malignant tumors and is the cause of approximately 90% of human cancer deaths.[1,2] Tumor metastasis is an exceedingly complex process, which occurs through a series of sequential steps that include dissociation from the primary tumor, invasion of adjacent tissues, intravasation, transport through the circulatory system, arrest in small vessels, adhesion to endothelial cells, extravasation and growth in secondary organs.[3] It can be hypothesized that components of the secondary organ, such as endothelial cells, stromal cells, fibroblasts and parenchymal cells, are functionally organized to promote survival and proliferation of metastasizing cancer cells and generate a favorable microenvironment for cancer cells in metastatic sites.[4,5]

Hypoxia initiates a variety of cellular responses including the activation of hypoxia-inducible factor-1 (HIF-1).[6,7] HIF-1 is a ubiquitously expressed heterodimeric transcription factor composed of a constitutively expressed β subunit and an oxygen-regulated α subunit. Under normal oxygen tension, the α subunit is continuously hydroxylated at conserved prolyl and asparaginyl residues and is targeted for degradation by the von Hippel–Lindau ubiquitin E3 ligase complex.[8] In hypoxia, inhibition of hydroxylation results in the stabilization of HIF-1α and its subsequent nuclear entry, which leads to transcriptional activation of target genes that stimulates angiogenesis, such as vascular endothelial growth factor (VEGF), that controls invasion of cancer cells, such as matrix metalloproteinases (MMPs), and promotes metabolic adaptation to hypoxia.[9] In general, tumor cells grow faster than the rate of angiogenesis so that tumor tissues are characterized by internal hypoxia. Therefore, activation of HIF-1 has been described in a variety of human cancers and their metastases.[10,11] Moreover, although the role of HIF-1α in tumor cell growth has not been fully elucidated, our results and those from other groups have demonstrated that HIF-1α expression in tumor tissues is likely to help tumor cell survival and growth.[12,13]

RNA interference (RNAi) is an evolutionary conserved sequence-specific gene silencing mechanism, which can be triggered by small 21- to 25-nt double-stranded small interfering RNA (siRNA) or short hairpin RNA (shRNA) that is processed in the cell to form siRNA.[14,15] Intravascular injection of a large-volume isotonic solution at a high speed is a very efficient method for delivering any solutes, including siRNA- and shRNA-expressing plasmid DNA (pDNA), to liver cells. This procedure, the so-called hydrodynamics-based procedure, has been applied to suppress expression of target genes in the liver.[16,17] In addition to such application, we found that the hydrodynamic

Correspondence: Professor Y Takakura, Department of Biopharmaceutics and Drug Metabolism, Graduate School of Pharmaceutical Sciences, Kyoto University, Sakyo-ku, Kyoto 606-8501, Japan.
E-mail: takakura@pharm.kyoto-u.ac.jp
Received 2 August 2007; revised 4 December 2007; accepted 5 December 2007

administration is also applicable to deliver siRNA- and shRNA-expressing pDNA to tumor cells in the liver.[18] Therefore, the hydrodynamics-based procedure can be an effective method to suppress the growth of tumor cells that are metastasized to the liver. Because the hydrodynamic administration can induce RNAi in both tumor cells in the liver and normal liver cells, suppressing the increased expression of a gene that aggravates the metastatic tumor growth in both tumor and liver cells can be an effective approach in treating hepatic metastasis. To this end, we selected HIF-1α as such a target gene in the present study. We applied the hydrodynamic injection method to administer shRNA-expressing pDNA targeting HIF-1α (pshHIF-1α) and found that the suppression of HIF-1α expression in the liver can suppress the growth of metastasizing tumor cells in that organ. Moreover, selective suppression of HIF-1α expression only in normal liver cells was found to be also effective in inhibiting metastatic tumor growth, indicating that HIF-1α expression in normal cells assisted the tumor progression.

Results

Reduction in protein expression of HIF-1α by shRNA-expressing pDNA

As previously reported by several groups, an enzyme-linked immunosorbent assay (ELISA) analysis showed that addition of $CoCl_2$ increased the amount of HIF-1α proteins in Colon26 and B16-BL6 cells (Figure 1a). Similar results were obtained when HIF-1α protein levels in Colon26 cells were evaluated by western blot analysis (Figure 1b). Transfection of pshHIF-1α reduced the amount of HIF-1α protein, whereas transfection of control pDNA or pshGFP (green fluorescent protein) hardly affected the level of HIF-1α expression.

Using immunofluorescent staining with HIF-1α-specific antibody, localization of HIF-1α protein in the cells was visualized. While a weak signal of HIF-1α was observed in cytoplasm when cells were incubated without $CoCl_2$, incubation of Colon26 cells with $CoCl_2$ resulted in nuclear accumulation of HIF-1α, which was detected as yellow signals as a result of overlap between the green fluorescence derived from HIF-1α and the red fluorescence derived from nuclear staining (Figure 1c). Transfection of pshHIF-1α reduced the number of cells that show HIF-1α accumulation in their nucleus.

Inhibition of HIF-1 transcriptional activity by pshHIF-1α

To investigate whether pshHIF-1α is effective in suppressing the transcription activity of HIF-1, cells were transfected with a pDNA encoding luciferase gene under the control of hypoxia response element (HRE). In Colon26 cells, HRE-dependent luciferase expression from the reporter pDNA co-transfected with control pDNA or pshGFP was moderately increased by the addition of $CoCl_2$. However, in B16-BL6 cells, HRE-dependent luciferase expression was increased by the addition of $CoCl_2$ compared with Colon26 cells (Figures 2a and b). HRE-dependent luciferase expression in the presence of $CoCl_2$ was almost completely inhibited to about the expression level observed in the absence of $CoCl_2$ by transfection of pshHIF-1α.

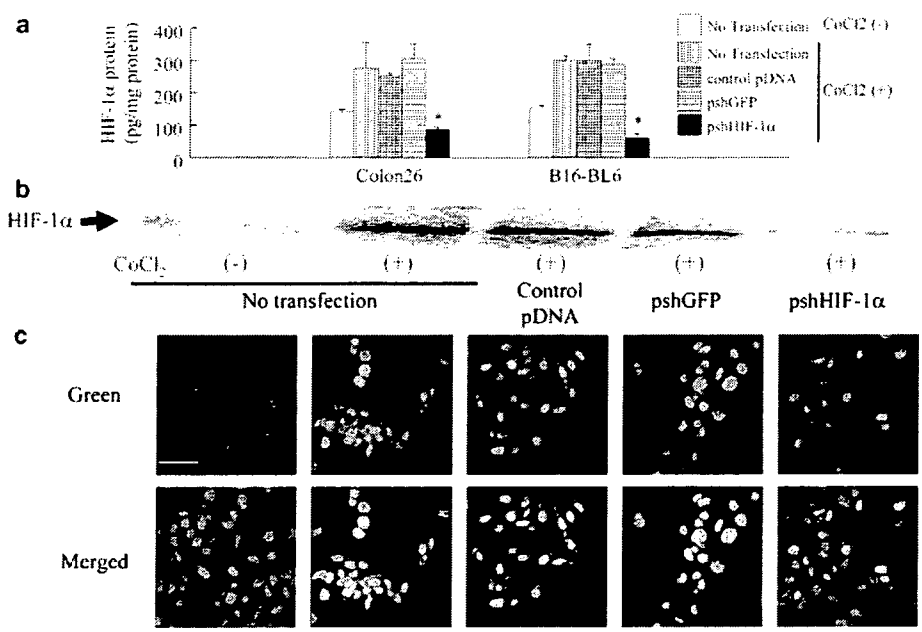

Figure 1 Hypoxia-inducible factor-1α (HIF-1α) protein expression level in tumor cells following transfection of short hairpin (shRNA)-expressing plasmid DNA (pDNA). Cells were transfected with control pDNA, pshGFP (green fluorescent protein) or pDNA expressing shRNA targeting HIF-1α (pshHIF-1α). At 4 h after transfection, cells were washed with phosphate-buffered saline (PBS) and then cultured with growth medium supplemented with or without 100 μM $CoCl_2$ for an additional 20 h. (**a**) Enzyme-linked immunosorbent assay (ELISA) analysis of HIF-1α protein from cell lysates of Colon26 or B16-BL6 cells. The results are expressed as the mean ± s.d. of three samples. $^*P < 0.05$ for Student's *t*-test versus the control group. (**b**) Western blotting analysis of HIF-1α for cell lysates of Colon26 cells. (**c**) Immunofluorescent staining of HIF-1α in transfected Colon26 cells. HIF-1α protein expression was detected as a green color, and the cell nucleus was stained with propidium iodide (red). Yellow signals indicate that HIF-1α localizes in the cell nucleus. Scale bar = 50 μm.

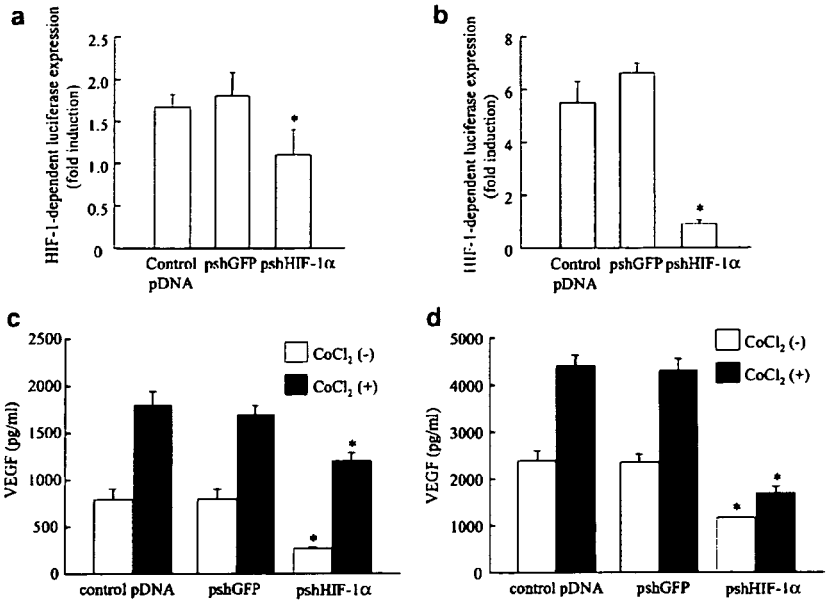

Figure 2 Suppression of hypoxia-inducible factor-1 (HIF-1)-dependent gene expression by transfection of plasmid DNA (pDNA) expressing shRNA targeting HIF-1α (pshHIF-1α). (**a**, **b**) Suppression of HIF-1-dependent reporter gene expression by pshHIF-1α. pLuc-HRE and phRL-TK were co-transfected with control pDNA, pshGFP (green fluorescent protein) or pshHIF-1α to Colon26 (**a**) or B16-BL6 (**b**) cells. At 4 h after transfection, cells were washed with phosphate-buffered saline (PBS) and cultured in medium with or without 100 μM $CoCl_2$ for an additional 20 h. Luciferase activities were measured 24 h after transfection. The results are expressed as the mean ± s.d. of three samples. (**c**, **d**) Reduction in HIF-1-dependent vascular endothelial growth factor (VEGF) production by pshHIF-1α. Colon26 (**c**) or B16-BL6 (**d**) cells were transfected with control pDNA, pshGFP or pshHIF-1α. At 4 h after transfection, cells were washed with PBS and cultured in medium with or without 100 μM $CoCl_2$ for an additional 44 h. The amount of VEGF protein in the cultured medium was measured 48 h after transfection using enzyme-linked immunosorbent assay (ELISA). The results are expressed as the mean ± s.d. of three samples. *$P<0.05$ for Student's *t*-test versus the control group.

To further estimate the effect of pshHIF-1α transfection on the expression of VEGF, an endogenous gene product of HIF-1 transcription activity, culture media of tumor cells were collected 48 h after the transfection. The VEGF concentration in the supernatant was measured by ELISA (Figures 2c and d). In both cell lines, about a two-fold increase was detected in the VEGF from $CoCl_2$-treated cells compared with that from untreated cells. In Colon26 cells, transfection of pshHIF-1α reduced VEGF secretion to about one-third or two-thirds of the control values without or with $CoCl_2$, respectively. In B16-BL6 cells, transfection of pshHIF-1α reduced VEGF secretion to about half or one-third of the control values without or with $CoCl_2$, respectively.

Increase in HIF-1α expression in the liver by tumor inoculation via the portal vein

Mice were inoculated with tumor cells into the portal vein, and received an intravenous injection of each pDNA 5 days after tumor inoculation. Then, immunofluorescent staining of liver sections was performed to detect HIF-1α protein expression 7 days after tumor inoculation. Representative images are shown in Figures 3a–g. No significant signal of HIF-1α was observed in the liver sections of naïve mice, sham-operated mice and those receiving control pDNA (Figures 3a–c). In contrast, a strong HIF-1α signal was observed in the liver sections of tumor-bearing mice (Figure 3d). In these pictures, increased HIF-1α expression was mainly observed in hepatic cells. Administration of control pDNA or pshGFP had little effect on HIF-1α expression induced by the inoculation of tumor cells (Figures 3e and f). Moreover, hydrodynamic administration of pshHIF-1α reduced the signal intensity derived from HIF-1α protein compared with other tumor-bearing groups (Figure 3g). By quantitatively analyzing relative areas of the HIF-1α expression (green signal) to the total area in the images, the percentage inhibition by pshHIF-1α was calculated to be about 20–30% of the other tumor-bearing groups. In addition, the administration of pshHIF-1α significantly ($P<0.05$) reduced the mRNA expression of HIF-1α in tumor-bearing liver, from 0.0059 ± 0.0011 copies relative to GAPDH mRNA (the control pDNA-treated group) to 0.0021 ± 0.0005.

Suppression of HIF-1α expression in liver by the pre-administration of pshHIF-1α

As it had been demonstrated that tumor inoculation via the portal vein induced HIF-1α accumulation in liver cells, we investigated whether the delivery of pshHIF-1α only to liver cells, not to tumor cells, affects tumor growth in the liver. To this end, tumor cells were inoculated 3 days after the hydrodynamic administration of pDNAs. Immunofluorescent staining for HIF-1α was performed at 2 days after tumor inoculation to investigate the HIF-1α expression level at that time (Figures 3h–l). Similar to the results of the sample prepared at 7 days after tumor inoculation, a strong signal derived from HIF-1α protein was detected in the liver sections prepared at 2 days after tumor inoculation (Figure 3i).

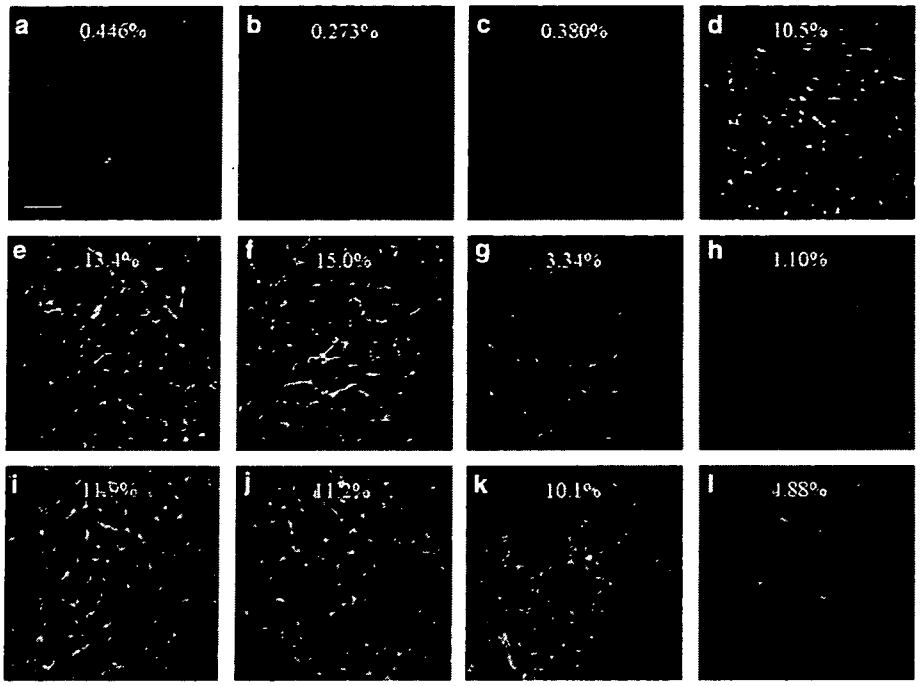

Figure 3 Hypoxia-inducible factor-1α (HIF-1α) expression in the liver of tumor-bearing mice. Some mice were untreated (**a**) or received plasmid DNA (pDNA) only (**b**). The sham operation group (**c**) received only an intraportal injection of Hank's balanced salt solution (HBSS) solution without tumor cells. At 5 days after tumor inoculation via the portal vein, mice were untreated (**d**) or received an intravenous injection of control pDNA (**e**), pshGFP (green fluorescent protein) (**f**) or pDNA expressing shRNA targeting HIF-1α (pshHIF-1α) (**g**). At 2 days after pDNA administration, liver samples were collected and subjected to immunostaining for HIF-1α. The sham operation group received only an intraportal injection of HBSS solution without tumor cells (**h**). At 3 days before tumor inoculation via the portal vein, mice were untreated (**i**) or received an intravenous injection of control pDNA (**j**), pshGFP (**k**) or pshHIF-1α (**l**). At 2 days after tumor inoculation, liver samples were collected and subjected to immunostaining for HIF-1α. Scale bar = 50 μm. Numbers in the images represent the relative area of HIF-1α expression (green signal) to the total area. See online version for color figure.

pshHIF-1α administrated before tumor inoculation suppressed the induction of HIF-1α expression by tumor inoculation (Figure 3l). Administration of irrelevant pDNAs did not change the expression level of HIF-1α in the liver (Figures 3j and k). Quantification of the relative areas of the HIF-1α expression (green signal) to the total area in the images indicated that pre-administration of pshHIF-1α reduced HIF-1α expression to about 50% of the other tumor-inoculated groups.

Location of HIF-1α expression in the tumor-inoculated liver relative to tumor cells

To visualize Colon26 cells in the liver, Colon26 cells transfected with pDsRed2-N1 were inoculated into the portal vein of mice. Immunofluorescent staining for HIF-1α was performed at 2 days after tumor inoculation to investigate the location of HIF-1α expression relative to tumor cells (Figures 4a–d). DsRed-labeled Colon26 cells were found in some liver sections, and almost all of these cells were surrounded by liver cells expressing an increased level of HIF-1α (Figures 4a and b). Some liver cells not close to Colon26 cells also showed a high HIF-1α expression (Figure 4c), but most other liver cells hardly expressed the protein (Figure 4d). These results suggest that tumor cells entrapped in the hepatic capillaries is closely associated with the increased expression of HIF-1α in the surrounding liver cells.

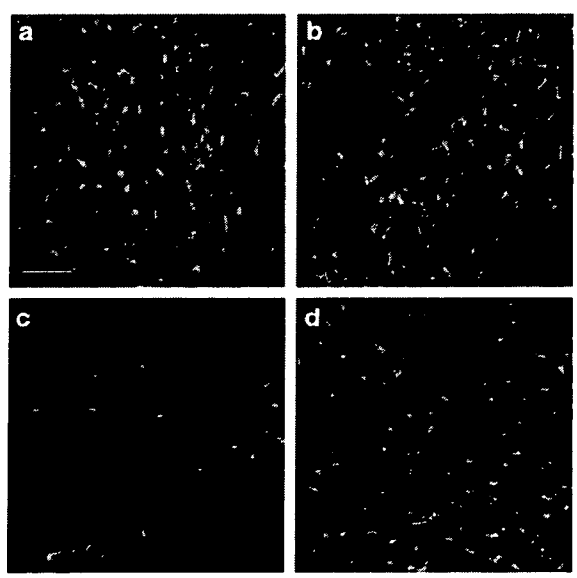

Figure 4 Location of hypoxia-inducible factor-1α (HIF-1α) expression in the tumor-bearing liver relative to tumor cells. At 2 days after tumor inoculation, liver samples were collected and subjected to immunostaining for HIF-1α. Red signals represent Colon26 cells expressing DsRed, and green signals represent HIF-1α protein. Representative images of liver sections positive (**a**, **b**) or negative (**c**, **d**) for DsRed-labeled Colon26 cells are indicated. Scale bar = 50 μm.

Induction of MMP-2 and -9 expression in the liver by tumor inoculation via the portal vein

To evaluate the effect of tumor inoculation via the portal vein on the MMP expression in the liver, the amount of MMP in liver homogenate was measured by gelatin zymography 8 days after tumor inoculation (Figure 5a). As we have reported previously, MMP-2 and -9 activities in the homogenate of tumor-inoculated liver was higher than that of the untreated group. A hydrodynamic delivery of control pDNA or pshGFP 5 days after tumor inoculation had little or no effect on both types of MMP activity. No significant increase in the MMP activity was detected in the liver homogenate of sham-operated mice or mice that received only pDNA. Intravenous injection of pshHIF-1α by the hydrodynamics-based procedure 5 days after tumor inoculation clearly reduced the MMP-9 gelatinolytic activity in the liver of tumor-bearing mice compared with the other tumor-inoculated group. Less, but detectable, reduction was also observed in the MMP-2 activity.

To assess the effect of HIF-1α expression in normal cells on MMP production, pshHIF-1α was administered 3 days before tumor inoculation. Gelatin zymography was performed at 3 days after tumor inoculation (Figure 5b). At this time point, the sham operation group showed slightly increased MMP-9 activity compared with naïve mice. Although the increase in MMP-9 expression level in the liver at this time was smaller than that detected at 8 days after tumor inoculation, the homogenate of tumor-bearing liver showed a higher MMP-9 activity than the other tumor-free groups. Pretreatment of pshHIF-1α reduced MMP-9 induction by tumor inoculation, while preinjection of control pDNA and

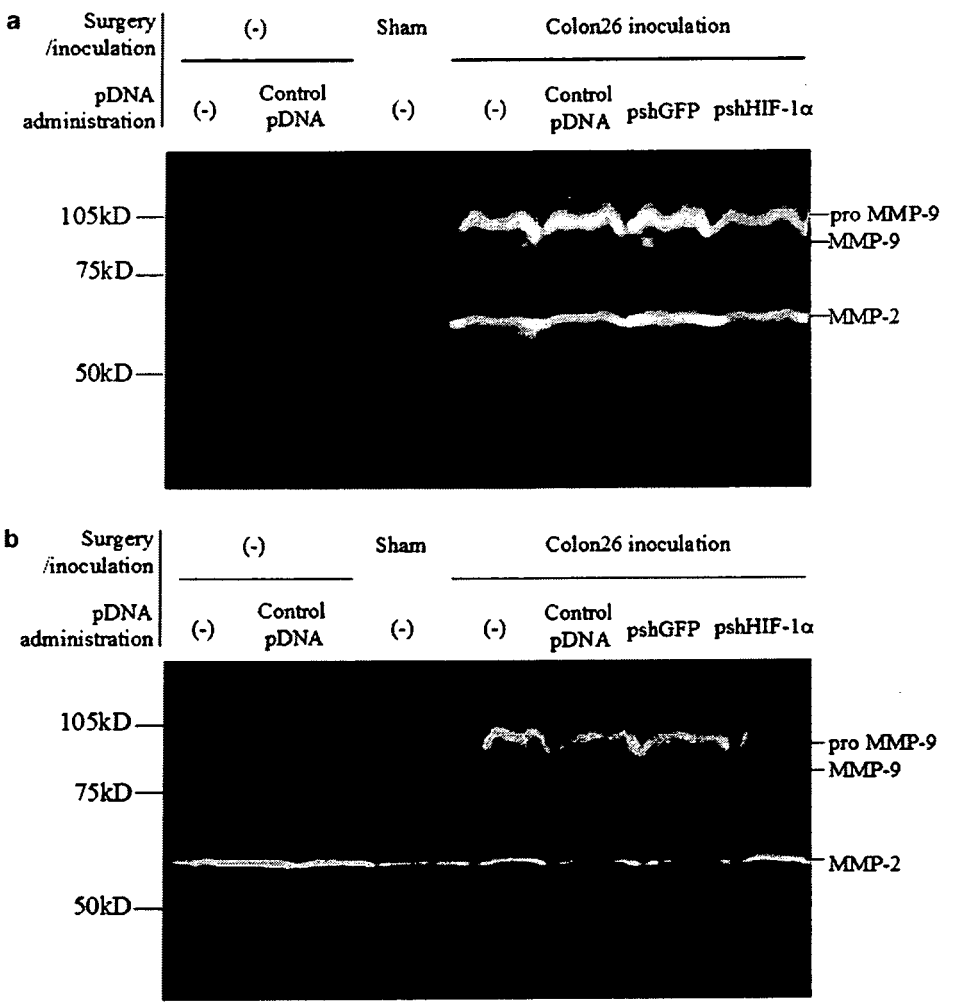

Figure 5 Gelatin zymography performed on liver samples. (a) At 5 days after tumor inoculation via the portal vein, mice received an intravenous injection of control plasmid DNA (pDNA), pshGFP (green fluorescent protein) or pDNA expressing shRNA targeting HIF-1α (pshHIF-1α). The sham operation group received only an intraportal injection of Hank's balanced salt solution (HBSS) solution without tumor cells. At 3 days after pDNA administration, liver samples were collected and subjected to gelatin gel zymography. Four mice of each group were used to analyze the matrix metalloproteinase (MMP) expression, and typical results are shown. (b) At 3 days before tumor inoculation via the portal vein, mice received an intravenous injection of control pDNA, pshGFP or pshHIF-1α. The sham operation group received only an intraportal injection of HBSS solution without tumor cells. At 3 days after tumor inoculation, liver samples were collected and subjected to gelatin gel zymography. Four mice of each group were used to analyze the MMP expression, and typical results are shown.

pshGFP had little effect on MMP-9 induction in the liver following tumor inoculation. We did not observe any obvious difference in MMP-2 production between tumor-free and tumor-bearing groups.

Suppression of metastatic tumor growth in the liver by pshHIF-1α

Figure 6a shows the tumor cell number in the liver, which was evaluated by measuring tumor-derived luciferase activities at 1 week after pDNA administration (Figure 6a). Mice were inoculated with Colon26 cells into the portal vein, and each pDNA was injected into the tail vein with 5-day interval. Control pDNA or pshGFP hardly reduced the number of tumor cells, while pshHIF-1α significantly ($P<0.05$) reduced the number to about, on average, 1–2% of the other groups. Many large tumor nodules were found in the frozen liver sections of mice receiving control pDNA (Figure 6c). In a quite contrast, much small and few tumor nodules were detected in the sections of mice receiving pshHIF-1α (Figure 6d). These hematoxylin and eosin-stained sections strongly support the quantitative results of metastatic tumor growth estimated using the luciferase activity of Colon26/Luc cells (Figure 6a).

Next, we investigated the effect of preadministration of pshHIF-1α on the growth of tumor cells in the liver by estimating the tumor cell number 12 days after tumor inoculation (Figure 6b). As a result, pshHIF-1α preadministration 3 days before tumor inoculation significantly reduced the number of tumor cells in the liver 12 days after tumor inoculation compared with the groups that were untreated or given pDNA. On average,

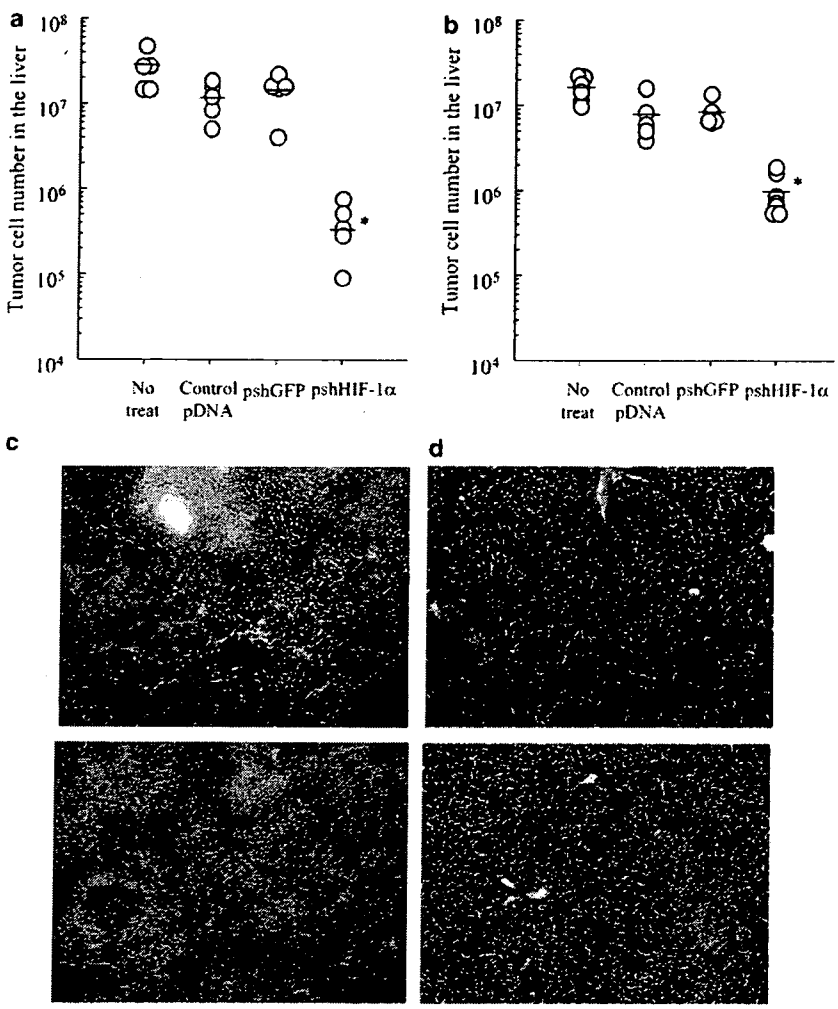

Figure 6 Number of Colon26/Luc cells in mouse liver 12 days after tumor inoculation. (**a**) At 5 days after tumor inoculation via the portal vein, mice received an intravenous injection of control plasmid DNA (pDNA), pshGFP (green fluorescent protein) or pDNA expressing shRNA targeting HIF-1α (pshHIF-1α). At 7 days after pDNA administration, liver samples were collected and the number of tumor cells was evaluated by measuring luciferase activities derived from Colon26/Luc cells. Open circles (○) indicate the tumor cell number in the liver of individual mice. Bars indicate the average tumor cell number of each group ($n=5$). *$P<0.05$ for Student's *t*-test versus untreated group. (**b**) At 3 days before tumor inoculation via the portal vein, mice received an intravenous injection of control pDNA, pshGFP or pshHIF-1α. At 12 days after tumor inoculation, liver samples were collected and the number of tumor cells was evaluated by measuring luciferase activities derived from Colon26/Luc cells. Open circles (○) indicate the tumor cell number in the liver of individual mice. Bars indicate the average tumor cell number of each group of at least five mice. *$P<0.05$ for Student's *t*-test versus untreated group. (**c**, **d**) Hematoxylin and eosin-stained liver sections of tumor-bearing mice receiving (**c**) control pDNA or (**d**) pshHIF-1α at 7 days after tumor inoculation. Scale bar = 200 μm. See online version for color figure.

preadministration of pshHIF-1α reduced the number of tumor cells to about 10% of other groups. The degree of reduction in the number of tumor cells by pshHIF-1α administered before tumor inoculation was about 5- to 10-fold less than that of pshHIF-1α administered after tumor inoculation.

Discussion

HIF-1α expression and subsequent HIF-1 activation in cancer cells play important roles in cancer progression by controlling the gene expression related to cancer cell proliferation, apoptosis and metastasis.[9] In the present study, we demonstrated that HIF-1α expression in normal hepatic cells is also increased by tumor cells entering the liver via the portal vein and that such HIF-1α expression aggravates tumor growth. Our results indicate the possibility of a novel therapeutic strategy for inhibiting metastatic tumor growth by silencing the HIF-1α expression in both normal and tumor cells.

Suppression of nuclear accumulation of HIF-1α by pshHIF-1α (Figure 1) was followed by inhibition of HIF-1-dependent transcription activities (Figure 2). In the experiment using pLuc-HRE, pshHIF-1α suppressed the transcription activity to almost the basal level in both Colon26 and B16-BL6 cells. Such an efficient inhibitory effect on luciferase expression might be because pLuc-HRE was co-transfected with pshHIF-1α, by which both pDNAs were delivered to the same cells. On the other hand, the suppressive effect of pshHIF-1α on VEGF production from B16-BL6 cells was much greater than that from Colon26 cells. Two factors may explain the difference in the efficiency of the inhibitory effect on VEGF production between B16-BL6 cells and Colon26 cells. One is the transfection efficiency of the pshHIF-1α. By using pDNA expressing enhanced green fluorescent protein (EGFP), we found that the transfection efficiency to B16-BL6 and Colon26 cells was about 80–90 and 70–80%, respectively, at 24 h after transfection (Y Takahashi *et al.*, unpublished data). Therefore, the difference in transfection efficiency between B16-BL6 and Colon26 cells may be one reason for the difference in suppressive effect on VEGF production by pshHIF-1α. The other reason for the difference in suppression in the two cell lines could be the contribution of HIF-1-dependent VEGF production to the total VEGF production. Other hypoxia-inducible transcriptional factors, such as HIF-2, are also known to be activated by $CoCl_2$ and increased HIF-2 expression might result in VEGF expression.[19]

When tumor cells were inoculated via portal vein, HIF-1α protein expression was increased in tumor-bearing liver (Figure 3). Inoculation of DsRed-labeled Colon26 cells clearly demonstrated that liver cells close to the tumor cells expressed HIF-1α at a high level (Figure 4). Oxygen concentration-dependent and -independent pathways might be considered as the mechanism for such an increase in HIF-1α expression. When tumor cells are inoculated via the portal vein, tumor cells are first arrested in small vessels, followed by extravasation, invasion of tissues and proliferation of tumor cells.[3] Therefore, blood flows would be, at least transiently, hindered by tumor cells, which could result in a reduction in the oxygen supply. In addition to hypoxia, other processes such as growth factor stimulation and cytokine stimulation are reported to increase HIF-1α expression and activate HIF-1-dependent transcription.[9,20] When tumor cells metastasize to the liver, expression of these secretary proteins might be induced and result in increased HIF-1α expression.

To distinguish the role of HIF-1α expressed in tumor cells from that in normal liver cells, pshHIF-1α was administered 3 days before tumor inoculation. As pDNA injected into the systemic circulation is very quickly degraded by nucleases and cleared by Kupffer and sinusoidal endothelial cells,[21] pDNA injected would have hardly any effects on the expression level of HIF-1α in Colon26/Luc cells. On the other hand, when pshHIF-1α was administered after tumor inoculation, pshHIF-1α might be delivered to both tumor and liver cells.[18] Therefore, pshHIF-1α administered before tumor inoculation might have been delivered only to normal cells in the liver, while pshHIF-1α administered after tumor inoculation might have been delivered to both tumor and normal cells in the liver.

In a previous study, we reported that Colon26 cell inoculation via the portal vein increased MMP-9 expression in the liver.[22] Elezkurtaj *et al.*[23] demonstrated that intrasplenic inoculation of CT-26 colon carcinoma cells, which form experimental liver metastases, increased MMP-2 and -9 expressions in liver tissue. In agreement with these results, we have found that MMP-9 is generated mainly from host cells, not the inoculated tumor cells (Y Takahashi *et al.*, unpublished data). There are some published papers reporting that MMP-9 expression is directly or indirectly regulated by HIF-1.[24–26] Therefore, we hypothesized that increased HIF-1 transcription activity in normal cells in the liver contributes to MMP-9 production induced by tumor cell inoculation. Intravenous administration of pshHIF-1α was effective in reducing the expression of MMP-9 after tumor inoculation, which indicates that HIF-1 expression in tumor cells and normal cells in the liver might play an important role in MMP-9 production. Moreover, administration of pshHIF-1α before tumor inoculation was found to be also effective in reducing the amount of MMP-9 in the liver. This result reinforces the hypothesis that normal cells in the liver, not tumor cells, are the major producer of MMP-9 and that MMP-9 expression is regulated by HIF-1. Although its role in metastatic tumor cell growth is still unclear, increased MMP expression is frequently accompanied by tumor metastasis and suppression of MMP expression could be used as a growth inhibitory treatment to prevent tumor metastasis.[23,27,28]

When pshHIF-1α was administered to tumor-bearing mice by the hydrodynamics-based procedure, a significant reduction in the number of tumor cells was observed (Figure 6a). This result indicates that HIF-1α expression in either tumor cells or hepatic normal cells or in both types of cells plays an important role in tumor progression. A histological study of the liver sections confirmed that the administration of pshHIF-1α significantly reduced the metastatic tumor growth in the liver (Figures 6c and d). Preadministration of pshHIF-1α reduced the tumor cell number in the liver at 12 days after tumor inoculation compared with the other groups (Figure 6b). This result implies that HIF-1α expression in the normal cells in the liver might play an important role in tumor cell growth in the liver, although the reduction

in the tumor cell number was modest compared with the case where the pshHIF-1α was administered after tumor inoculation. As demonstrated in our previous study, hydrodynamic delivery of pDNA can deliver pDNA to tumor cells in the liver. Moreover, we and other groups have reported that intratumoral expression of HIF-1α helps cancer cell survival and proliferation as well as angiogenesis and cancer metastasis. Therefore, hydrodynamic administration of pshHIF-1α could suppress HIF-1α expression in tumor cells, which might also act as an inhibitory treatment to prevent tumor progression. When HIF-1α expression is increased in normal cells, it might result in upregulation of genes that can assist tumor cell growth and progression. In the present study, we focused on MMP-9 as an HIF-1-dependent tumor supportive protein produced from normal cells. Normal cells, including hepatocytes, have significantly fewer genetic mutations than cancer cells. Therefore, inhibiting the increase in HIF-1α expression in hepatocytes would have less chance of inducing resistance to treatment.

In conclusion, this study suggests that HIF-1α expression is increased in normal liver cells as well as cancerous cells, and HIF-1α expression plays an important role in tumor progression. RNAi of HIF-1 is an effective strategy for inhibiting tumor cell growth, and both tumor and normal cells can be targets for RNAi-based anticancer treatment.

Materials and methods

Plasmid DNA

Short hairpin-expressing pDNAs targeting GFP or HIF-1α were constructed from piGENE hU6 vector (iGENE Therapeutics, Tsukuba, Japan) as described previously.[18] Target sites in GFP and murine HIF-1α genes are as follows: GFP, 5′-GGCTACGTCCAGGAGCGCA-3′ and HIF-1α, 5′-GACACAGCCTCGATATGAA-3′. These pDNAs transcribe a stem-loop-type RNA with a loop sequence of ACGUGUGCUGUCCGU. In a previous study, we confirmed that transfection of pshHIF-1α suppresses the mRNA expression of HIF-1α in cultured cells.[13] piGENE hU6 vector, which transcribes a non-related sequence of RNA with partial duplex formation, was used as a control pDNA throughout the present study.

pDsRed2-N1 encoding red fluorescent protein Dsred2 was purchased from BD Biosciences Clontech (Palo Alto, CA, USA). pGL4.74[hRluc/TK] (phRL-TK) encoding sea pansy luciferase under the control of herpes simplex virus TK promoter was purchased from Promega (Madison, WI, USA). A HRE reporter plasmid encoding firefly luciferase (pLuc-HRE) was generated by subcloning nine copies of the HRE (5′-TACGTGCTGC-3′) from mouse erythropoietin enhancer into *Bgl*II/*Hin*dIII site of pLuc-MCS plasmid (Stratagene, La Jolla, CA, USA).

Each pDNA was amplified in the DH5α strain of *Escherichia coli* and purified by using a Qiagen Endofree Plasmid Giga Kit (Qiagen GmbH, Hilden, Germany).

Cell culture

A murine colon carcinoma cell line Colon26, obtained from the Cancer Chemotherapy Center of the Japanese Foundation for Cancer Research (Tokyo, Japan), and Colon26 cells that stably express firefly luciferase (Colon26/Luc)[29] were cultured in RPMI 1640 medium supplemented with 10% fetal bovine serum (FBS) and penicillin/streptomycin/L-glutamine at 37 °C and 5% CO_2. A murine melanoma cell line B16-BL6 cells[30], obtained from the Cancer Chemotherapy Center of the Japanese Foundation for Cancer Research, were cultured in Dulbecco's modified Eagle's minimum essential medium (DMEM; Nissui Pharmaceutical, Tokyo, Japan) supplemented with 10% FBS and penicillin/streptomycin/L-glutamine at 37 °C and 5% CO_2. To mimic hypoxic conditions and induce HIF-1α protein expression, cells were incubated with the culture medium supplemented with 100 μM $CoCl_2$.[31]

In vitro *transfection*

Tumor cells were plated on culture plates. After an overnight incubation, transfection of pDNA was carried out using Lipofectamine 2000 (Invitrogen, Carlsbad, CA, USA) according to the manufacturer's instructions. In brief, 1 μg pDNA was mixed with 3 μg Lipofectamine 2000 at a final concentration of 2 μg pDNA ml^{-1} dissolved in OPTI-MEM I (Invitrogen). The resulting complex was added to the cells and the cells were incubated with the complex for 4 h. Cells were washed with PBS and further incubated with the culture medium supplemented with or without 100 μM $CoCl_2$ for the indicated periods.

Detection of HIF-1α protein expression by western blotting and ELISA

At 24 h after transfection, total proteins were collected from Colon26 and B16-BL6 cells. For total protein extraction, cells were lysed in a lysis buffer containing 50 mM Tris (pH 7.4), 1% NP40, 0.25% Na-deoxycholate, 0.1% SDS, 150 mM NaCl, 1 mM EDTA, 1 mM PMSF, 1 mM NaF and 0.2% Sigma protease inhibitor cocktail (Sigma Aldrich, St Louis, MO, USA). The lysate was centrifuged at 13 000 *g* for 20 min at 4 °C and the supernatant was collected and used as a protein sample. Protein concentrations were determined using a Proteostain Protein Quantification Kit (Dojindo Molecular Technologies Inc., Tokyo, Japan).

For western blotting, 50 μg protein was diluted with a loading buffer, denatured at 95 °C for 3 min, and resolved by SDS-polyacrylamide gel electrophoresis (SDS-PAGE) (6.5% polyacrylamide) and transferred to a polyvinylidene fluoride membrane (Immobilon-P; Millipore Corp., Bedford, MA, USA) by semidry blotting with Transblot SD (Bio-Rad, Hercules, CA, USA). To avoid nonspecific binding, the membrane was incubated in 5% bovine serum albumin. Then HIF-1α protein was detected by a primary monoclonal mouse antibody against HIF-1α (1:500; Novus Biologicals, Littleton, CO, USA) and a secondary peroxidase-conjugated rabbit anti-mouse IgG antibody (1:2000; Amersham Biosciences Inc., Piscataway, NJ, USA). Protein bands were visualized by chemiluminescence on the ECL Plus protein detection system (Amersham Biosciences).

Concentrations of HIF-1α in the samples from tumor cells treated with or without $CoCl_2$ were measured by an ELISA kit (DuoSet IC; R&D Systems, Minneapolis, MN, USA) according to manufacturer's protocol.

HIF-1-dependent reporter gene expression assay

Tumor cells seeded on culture plates were transfected with pLuc-HRE (0.8 μg ml^{-1}), phRL-TK (0.2 μg ml^{-1}) and a control pDNA, pshHIF-1α or pshGFP (1 μg ml^{-1}) using Lipofectamine 2000 as described above. At 4 h after transfection, cells were washed with PBS and further incubated with the culture medium with or without 100 μM $CoCl_2$ for an additional 20 h. Then cells were lysed using Promega passive lysis buffer (Promega). Samples were mixed with dual-luciferase reporter system (Promega) and the chemiluminescence produced was measured in a luminometer (Lumat LB9507; EG and G Berthold, Bad Wildbad, Germany). The results were calculated as the activity of firefly luciferase relative to that of sea pansy luciferase to correct for differences in transfection efficiency. The ratios of $CoCl_2$-treated cells were normalized to give *x*-fold values relative to those of the corresponding untreated group.

Animals

Four-week-old male BALB/c mice (approximately 20 g body weight), purchased from Shizuoka Agricultural Cooperative Association (Shizuoka, Japan), were used in all experiments. All animal experiments were conducted in accordance with the principles and procedures outlined in the US National Institutes of Health Guide for the Care and Use of Laboratory Animals. The protocols for animal experiments were approved by the Animal Experimentation Committee of the Graduate School of Pharmaceutical Sciences of Kyoto University.

Hepatic metastasis of tumor cells

Colon26/Luc cells in an exponential growth phase were harvested by trypsinization and suspended in Hank's balanced salt solution (HBSS; Nissui Pharmaceutical). Under ether anesthesia, a midline abdominal incision was made to expose the portal vein, and 1×10^5 Colon26/Luc cells were injected into the portal vein. Then the opening was sutured and mice were allowed to recover. At 5 days after tumor inoculation, mice received an intravenous injection of pDNA at a dose of 2.5 mg kg^{-1} body weight. The intravenous injection was performed by the hydrodynamics-based procedure where pDNA dissolved in saline in a volume of 8% of the body weight was injected into the tail vein within less than 5 s using a 26-gauge needle.[32]

To evaluate the effect of HIF-1α expression in normal liver cells on the growth of tumor cells in the liver, mice received a hydrodynamic delivery of pDNA, followed by inoculation of tumor cells into the portal vein after an interval of 3 days.

To visualize the location of Colon26 cells in the liver, Colon26 cells labeled with a red fluorescent protein, DsRed, were used instead of Colon26/Luc cells. DsRed2-labeled Colon26 cells were prepared by transfecting cells with pDsRed2-N1, and inoculated into mice 24 h after transfection.

Immunofluorescent staining of HIF-1α

To visualize HIF-1α expression in cultured cells, immunofluorescent staining of HIF-1α was carried out. At 24 h after transfection, cells were fixed with 4% paraformaldehyde in PBS. The cell membrane was permeabilized by PBS containing 0.1% Triton X-100. After blocking with 10% FBS in PBS, cells were incubated with a monoclonal mouse antibody against HIF-1α (1:500; Novus Biologicals). After washing, Alexa Fluor 488 goat anti-mouse secondary antibody (1:600; Molecular Probes, Invitrogen) was added. Nuclear staining was performed using propidium iodide staining solution (50 μg ml^{-1} propidium iodide and 1 μg ml^{-1} RNase A in PBS). Slides were prepared using a SlowFade Antifade Kit (Molecular Probes). Samples were examined using a confocal laser microscope (MRC-1024; Bio-Rad).

For the detection of HIF-1α expression in the liver, mice under ether anesthesia were euthanized by cutting the vena cava, and the liver was gently infused with 2 ml saline through the portal vein to remove the remaining blood in the organ. The liver was then placed in Tissue-Tek OCT embedding compound (Sakura Finetechnical Co Ltd, Tokyo, Japan), frozen in liquid nitrogen, and stored in 2-methyl butanol at −80 °C until use. Frozen liver sections (8 μm thick) were obtained with a cryostat (Jung CM 3000; Leica Microsystems AG, Wetzlar, Germany) using a routine procedure. Sections were stained with HIF-1α-specific antibody by the same procedure as cultured cells except for the blocking process. Liver sections were blocked using the Vector M.O.M Immunodetection Kit (Vector Laboratories, Burlingame, CA, USA). Sections were examined using a confocal laser microscope. Relative areas of the HIF-1α expression (green signal) to the total area in the images were quantitatively analyzed by using a BZ-Analyzer software (KEYENCE, Osaka, Japan).

Gelatin zymography

At 3 or 8 days after tumor inoculation, mice under ether anesthesia were euthanized by cutting the vena cava. The liver was gently infused with 2 ml saline through the portal vein to remove the remaining blood. The liver was excised and homogenized in 5 ml g^{-1} lysis buffer (0.1 M Tris (pH 7.8), 0.05% Triton-X-100). The homogenate was centrifuged at 13 000 *g* for 20 min at 4 °C, then the supernatant was collected. For the measurement of gelatinase activity, 500 μg protein was electrophoresed under non-reducing conditions on 10% SDS-polyacrylamide gel containing 0.1% gelatin. Gels were washed twice for 30 min in 2.5% Triton X-100 and once for 30 min in 10 mM Tris-HCl (pH 8.0) and incubated overnight in 50 mM Tris-HCl (pH 8.0) containing 10 mM $CaCl_2$ and 10 nM $ZnCl_2$. The gels were then stained with 0.2% Coomasie brilliant blue and destained in 5% methanol and 7% acetic acid.

VEGF ELISA assay

To determine VEGF production in culture supernatants *in vitro*, tumor cells seeded on culture plates were transfected as described above and supernatants were collected for ELISA 48 h after the transfection. VEGF protein levels in the supernatant were measured using mouse VEGF-specific ELISA (Quantikine; R&D systems).

Inhibitory effect of pshHIF-1α on tumor growth in the liver

At 12 days after tumor inoculation, mice were euthanized by cervical dislocation and the liver was excised and homogenized in a lysis buffer (0.1 M Tris (pH 7.8), 0.05% Triton X-100, 2 mM EDTA), and centrifuged at

13 000 *g* for 20 min at 4 °C. The supernatant was mixed with a luciferase assay buffer (Picagene; Toyo Ink, Tokyo, Japan), and the light produced was measured with a luminometer (Lumat LB 9507). The luciferase activity of the liver was converted to the number of Colon26/Luc cells using a regression line as previously reported.[29] Different sets of mice were used for the histological evaluation of tumor-bearing livers. At 12 days after tumor inoculation, frozen liver sections were made as described above and stained with hematoxylin and eosin, followed by an examination using a microscope (Biozero BZ-8000; KEYENCE).

Statistical analysis

Experiments were performed at least in duplicate, and a typical set of data was indicated. Differences were statistically evaluated by Student's *t*-test. A *P*-value of less than 0.05 was considered to be statistically significant.

Acknowledgements

This study was supported in part by Grants-in-Aid for Scientific Research from the Ministry of Education, Science, Sports, and Culture of Japan, by grants from the Ministry of Health, Labour and Welfare of Japan and by a Grant-in-Aid for Exploratory Research from the Japan Society for the Promotion of Sciences.

References

1 Fidler IJ. Critical determinants of metastasis. *Semin Cancer Biol* 2002; **12**: 89–96.
2 Weigelt B, Peterse JL, van't Veer LJ. Breast cancer metastasis: markers and models. *Nat Rev Cancer* 2005; **5**: 591–602.
3 Engers R, Gabbert HE. Mechanisms of tumor metastasis: cell biological aspects and clinical implications. *J Cancer Res Clin Oncol* 2000; **126**: 682–692.
4 Olaso E, Santisteban A, Bidaurrazaga J, Gressner AM, Rosenbaum J, Vidal-Vanaclocha F. Tumor-dependent activation of rodent hepatic stellate cells during experimental melanoma metastasis. *Hepatology* 1997; **26**: 634–642.
5 Liotta LA, Kohn EC. The microenvironment of the tumour–host interface. *Nature* 2001; **411**: 375–379.
6 Wang GL, Semenza GL. General involvement of hypoxia-inducible factor 1 in transcriptional response to hypoxia. *Proc Natl Acad Sci USA* 1993; **90**: 4304–4308.
7 Wenger RH. Cellular adaptation to hypoxia: O_2-sensing protein hydroxylases, hypoxia-inducible transcription factors, and O_2-regulated gene expression. *FASEB J* 2002; **16**: 1151–1162.
8 Salceda S, Caro J. Hypoxia-inducible factor 1alpha (HIF-1alpha) protein is rapidly degraded by the ubiquitin–proteasome system under normoxic conditions. Its stabilization by hypoxia depends on redox-induced changes. *J Biol Chem* 1997; **272**: 22642–22647.
9 Semenza GL. Targeting HIF-1 for cancer therapy. *Nat Rev Cancer* 2003; **3**: 721–732.
10 Zhong H, De Marzo AM, Laughner E, Lim M, Hilton DA, Zagzag D *et al*. Overexpression of hypoxia-inducible factor 1alpha in common human cancers and their metastases. *Cancer Res* 1999; **59**: 5830–5835.
11 Talks KL, Turley H, Gatter KC, Maxwell PH, Pugh CW, Ratcliffe PJ *et al*. The expression and distribution of the hypoxia-inducible factors HIF-1alpha and HIF-2alpha in normal human tissues, cancers, and tumor-associated macrophages. *Am J Pathol* 2000; **157**: 411–421.
12 Li L, Lin X, Staver M, Shoemaker A, Semizarov D, Fesik SW *et al*. Evaluating hypoxia-inducible factor-1alpha as a cancer therapeutic target via inducible RNA interference *in vivo*. *Cancer Res* 2005; **65**: 7249–7258.
13 Takahashi Y, Nishikawa M, Takakura Y. Suppression of tumor growth by intratumoral injection of short hairpin RNA-expressing plasmid DNA targeting beta-catenin or hypoxia-inducible factor 1alpha. *J Control Release* 2006; **116**: 90–95.
14 Elbashir SM, Harborth J, Lendeckel W, Yalcin A, Weber K, Tuschl T. Duplexes of 21-nucleotide RNAs mediate RNA interference in cultured mammalian cells. *Nature* 2001; **411**: 494–498.
15 Brummelkamp TR, Bernards R, Agami R. A system for stable expression of short interfering RNAs in mammalian cells. *Science* 2002; **296**: 550–553.
16 McCaffrey AP, Meuse L, Pham T-TT, Conklin DS, Hannon GJ, Kay MA. RNA interference in adult mice. *Nature* 2002; **418**: 38–39.
17 Song E, Lee SK, Wang J, Ince N, Ouyang N, Min J *et al*. RNA interference targeting Fas protects mice from fulminant hepatitis. *Nat Med* 2003; **9**: 347–351.
18 Takahashi Y, Nishikawa M, Kobayashi N, Takakura Y. Gene silencing in primary and metastatic tumors by small interfering RNA delivery in mice: quantitative analysis using melanoma cells expressing firefly and sea pansy luciferases. *J Control Release* 2005; **105**: 332–343.
19 Carroll VA, Ashcroft M. Role of hypoxia-inducible factor (HIF)-1alpha versus HIF-2alpha in the regulation of HIF target genes in response to hypoxia, insulin-like growth factor-I, or loss of von Hippel–Lindau function: implications for targeting the HIF pathway. *Cancer Res* 2006; **66**: 6264–6270.
20 Mazure NM, Brahimi-Horn MC, Berta MA, Benizri E, Bilton RL, Dayan F *et al*. HIF-1: master and commander of the hypoxic world. A pharmacological approach to its regulation by siRNAs. *Biochem Pharmacol* 2004; **68**: 971–980.
21 Kawabata K, Takakura Y, Hashida M. The fate of plasmid DNA after intravenous injection in mice: involvement of scavenger receptors in its hepatic uptake. *Pharm Res* 1995; **12**: 825–830.
22 Nishikawa M, Tamada A, Hyoudou K, Umeyama Y, Takahashi Y, Kobayashi Y *et al*. Inhibition of experimental hepatic metastasis by targeted delivery of catalase in mice. *Clin Exp Metastasis* 2004; **21**: 213–221.
23 Elezkurtaj S, Kopitz C, Baker AH, Perez-Cantó A, Arlt MJ, Khokha R *et al*. Adenovirus-mediated overexpression of tissue inhibitor of metalloproteinases-1 in the liver: efficient protection against T-cell lymphoma and colon carcinoma metastasis. *J Gene Med* 2004; **6**: 1228–1237.
24 Krishnamachary B, Berg-Dixon S, Kelly B, Agani F, Feldser D, Ferreira G *et al*. Regulation of colon carcinoma cell invasion by hypoxia-inducible factor 1. *Cancer Res* 2003; **63**: 1138–1143.
25 Shi YF, Fong CC, Zhang Q, Cheung PY, Tzang CH, Wu RS *et al*. Hypoxia induces the activation of human hepatic stellate cells LX-2 through TGF-beta signaling pathway. *FEBS Lett* 2007; **581**: 203–210.
26 Stuelten CH, DaCosta Byfield S, Arany PR, Karpova TS, Stetler-Stevenson WG, Roberts AB. Breast cancer cells induce stromal fibroblasts to express MMP-9 via secretion of TNF-alpha and TGF-beta. *J Cell Sci* 2005; **118**: 2143–2153.
27 Waas ET, Wobbes T, Lomme RM, DeGroot J, Ruers T, Hendriks T. Matrix metalloproteinase 2 and 9 activity in patients with colorectal cancer liver metastasis. *Br J Surg* 2003; **90**: 1556–1564.
28 Lakka SS, Rajan M, Gondi C, Yanamandra N, Chandrasekar N, Jasti SL *et al*. Adenovirus-mediated expression of antisense MMP-9 in glioma cells inhibits tumor growth and invasion. *Oncogene* 2002; **21**: 8011–8019.
29 Kuramoto Y, Nishikawa M, Hyoudou K, Yamashita F, Hashida M. Inhibition of peritoneal dissemination of tumor cells by single dosing of phosphodiester CpG oligonucleotide/cationic liposome complex. *J Control Release* 2006; **115**: 226–233.

30 Poste G, Doll J, Hart IR, Fidler IJ. *In vitro* selection of murine B16 melanoma variants with enhanced tissue-invasive properties. *Cancer Res* 1980; **40**: 1636–1644.
31 Gray MJ, Zhang J, Ellis LM, Semenza GL, Evans DB, Watowich SS *et al*. HIF-1alpha, STAT3, CBP/p300 and Ref-1/APE are components of a transcriptional complex that regulates Src-dependent hypoxia-induced expression of VEGF in pancreatic and prostate carcinomas. *Oncogene* 2005; **24**: 3110–3120.
32 Liu F, Song Y, Liu D. Hydrodynamics-based transfection in animals by systemic administration of plasmid DNA. *Gene Ther* 1999; **6**: 1258–1266.

Available online at www.sciencedirect.com
ScienceDirect
Journal of Biotechnology 133 (2008) 36–41
Journal of BIOTECHNOLOGY
www.elsevier.com/locate/jbiotec

Insertion of nuclear factor-κB binding sequence into plasmid DNA for increased transgene expression in colon carcinoma cells

Oranuch Thanaketpaisarn[a], Makiya Nishikawa[b,*], Takayuki Okabe[a], Fumiyoshi Yamashita[a], Mitsuru Hashida[a]

[a] *Department of Drug Delivery Research, Graduate School of Pharmaceutical Sciences, Kyoto University, Sakyo-ku, Kyoto 606-8501, Japan*
[b] *Department of Biopharmaceutics and Drug Metabolism, Graduate School of Pharmaceutical Sciences, Kyoto University, Sakyo-ku, Kyoto 606-8501, Japan*

Received 14 May 2007; received in revised form 20 August 2007; accepted 25 August 2007

Abstract

To increase plasmid DNA (pDNA)-based transgene expression, 5, 10 or 20 repeats of nuclear factor κB (NF-κB) binding sequences were inserted upstream of the cytomegalovirus (CMV) promoter region of a conventional pDNA encoding firefly luciferase (pCMV-Luc) to obtain pCMV-κB5-Luc, pCMV-κB10-Luc and pCMV-κB20-Luc. Murine carcinoma colon 26 cells, in which NF-κB was constitutively activated, were co-transfected with a firefly luciferase-expressing pDNA and a renilla luciferase-expressing pDNA having no NF-κB binding sequences using cationic liposomes. The expression efficiency of pCMV-κB(*n*)-Luc was evaluated using the ratio of the luciferase activities. Increasing numbers of NF-κB binding sequences significantly increased transgene expression. The expression was increased by NF-κB activators and the effects were marked with pDNA having many NF-κB binding sequences. These results indicate that insertion of NF-κB binding sequences into pDNA is an effective approach to increase transgene expression in cancer cells in which NF-κB is activated.

Keywords: Gene transfer; Transcription factor; Nuclear factor-κB; Reactive oxygen species; Colon carcinoma cell; Nuclear transport

1. Introduction

The final delivery barrier in plasmid DNA (pDNA)-mediated gene transfer is the passage through the nuclear membrane. Because the threshold size for DNA to freely pass through the nuclear pore complex (NPC) is a molecular weight of about 50 kDa, or between 200 and 310 bp in length (Ludtke et al., 1999). pDNA is generally too large to pass, unassisted, through the NPC. Therefore, pDNA is believed to enter the nucleus when the nuclear membrane structure disappears during the M-phase of mitosis (Moritimer et al., 1999; Tseng et al., 1999). Nuclear translocation has been reported to be the rate-limiting step in the gene transfer process rather than the cell entry (Zhou et al., 2004). Lack of an efficient translocation of pDNA into the nucleus through the NPC, where it is transcribed, results in unacceptably low levels of transgene expression by most nonviral gene transfer methods. Nonviral vectors, such as cationic lipids (liposomes) and polymers, could protect pDNA from nuclease degradation, and improve its cellular entry, but they may not assist pDNA in its nuclear entry, because pDNA is eventually released from the complexes before entering the nucleus (Zabner et al., 1995; Xu and Szoka, 1996).

Dean et al. demonstrated that any eukaryotic promoter, enhancer, insulator, or regulatory specific sequence plays important roles in the nuclear targeting of DNA (Dean et al., 2005); following cytoplasmic microinjection, pDNA is translocated into the nucleus in association with several types of transcription factors (Dean, 1997; Dean et al., 1999). One of the most important transcription factors in the nuclear entry of pDNA is nuclear factor κB (NF-κB). NF-κB protein localizes in the cytoplasm in a bound form with its inhibitory protein, IκB, which shields the nuclear localization signal of NF-κB. Once cells are exposed to any signal that activates NF-κB, specific IκB family members rapidly undergo stimulus-coupled phosphorylation,

Abbreviations: pDNA, plasmid DNA; NF-κB, nuclear factor κB; NPC, nuclear pore complex; ROS, reactive oxygen species; CMV, cytomegalovirus; PMS, phenazine methosulfate.

* Corresponding author. Tel.: +81 75 753 4580; fax: +81 75 753 4614.
E-mail address: makiya@pharm.kyoto-u.ac.jp (M. Nishikawa).

0168-1656/$ – see front matter © 2007 Elsevier B.V. All rights reserved.
doi:10.1016/j.jbiotec.2007.08.047

ubiquitination and proteasome-mediated degradation, resulting in the liberation of active NF-κB heterodimers. After entering the nucleus, the activated NF-κB can bind specifically to its corresponding NF-κB binding sequence in DNA, leading to enhanced transcription and expression of downstream genes (Pahl, 1999). It has also been reported that pDNA can be translocated into the nucleus by inserting NF-κB binding sequences (Mesika et al., 2001). In a previous study, we demonstrated that an intravenous injection of pDNA/cationic liposome complex (lipoplex) activated the NF-κB in mouse lung, and this activation can be used to enhance lipoplex-mediated transgene expression by inserting NF-κB binding sequences into pDNA (Kuramoto et al., 2006).

These pieces of evidence suggest that the NF-κB activity of cells, which is a function of various physiological conditions, influences the level of transgene expression by pDNA-based gene transfer. Abnormally high NF-κB activity can be found in affected organs of patients with rheumatoid arthritis, asthma and inflammatory bowel disease (Kumar et al., 2004), as well as in acute lymphoblastic leukemia, breast cancer and diverse solid tumor-derived cell lines (Visconti et al., 1997). NF-κB is generally thought to be involved in the primary oxidative stress–response, acting as a redox-sensitive transcription factor. Reactive oxygen species (ROS) can function as components of signal transduction cascades in many cellular processes and act as common second messengers following cellular exposure to agents that induce NF-κB activation (Gius et al., 1999). ROS, such as hydrogen peroxide, have been reported to induce NF-κB activation in some types of cells (Mercurio and Manning, 1999; Bowie and O'Neill, 2000) and are signal molecules that play important roles in tumor growth and metastasis (Zhu et al., 2002; Rhee, 1999; Yoon et al., 2002).

In this study, to increase the transgene expression by nonviral vectors for cancer gene therapy, we first examined whether NF-κB is activated in colon carcinoma cells and whether this activation can be further increased by the treatment of cells with phenazine methosulfate (PMS) or hydrogen peroxide. Then, we designed new pDNA constructs by inserting NF-κB binding sequences to a conventional pDNA and examined whether the addition of the sequences is effective in increasing transgene expression. We propose here that the insertion of a suitable number of NF-κB binding sequences into pDNA is an effective approach to increasing transgene expression in cells in which NF-κB is transiently or constitutively activated.

2. Materials and methods

2.1. Chemicals

PathDetect® NF-κB *cis*-reporting pNF-κB-Luc plasmid was purchased from Stratagene (La Jolla, CA). Plasmid DNA encoding renilla luciferase under the control of SV40 promoter (pSV40-RL) was purchased from Promega (Madison, WI). Oligonucleotides were purchased from Nihon Gene Research (Sendai, Japan); a pair with a consensus NF-κB binding sequence (5′-TCAGAGGGGACTTTCCGAGAGG-3′ and 3′-AGTCTCCCCTGAAAGGCTCTCC-5′, the underlined part represents an NF-κB binding sequence) and another pair without the binding sequence (5′-AGTGTCAGCACGTGGAGATGCG-3′ and 3′-TCACAGTCGTGCACCTCTACGC-5′). [γ-^{32}P]ATP was purchased from Amersham (Tokyo, Japan). Lipofectamine2000 was purchased from GIBCO-Invitrogen (Carlsbad, CA). Opti-MEM® was obtained from Gibco BRL (Grand Island, NY). Dual-Luciferase™ Reporter Assay was purchased from Wako Pure Chemical (Osaka, Japan). All other chemicals were of the highest purity available.

2.2. Preparation of pDNA constructs

pCMV-Luc was constructed by inserting the firefly luciferase cDNA fragment from pGL3-control vector (Promega, Madison, WI) into the HindIII/XbaI site of pcDNA3 vector (Invitrogen, Carlsbad, CA) as previously reported (Sakurai et al., 2001). pCMV-κB(*n*)-Luc ($n = 5$, 10 or 20) was constructed as follows. The five repeats of the NF-κB binding sequence were amplified from pNF-κB-Luc by PCR using a set of primers (5′-primer, GAAGATCTATGTCTGGATCCAAGCTA; 3′-primer, TGTTCGCGAATACCCTCTAGAGTCACC) containing the BglII (5′-end) and NruI (3′-end) site, then the PCR product was digested with the restriction enzymes. Then, the DNA fragment was cloned into the BglII/NruI site of pCMV-Luc to obtain pCMV-κB5-Luc as reported previously (Kuramoto et al., 2006). To construct pCMV-κB10-Luc, the five repeats of the NF-κB binding sequence were amplified from pCMV-κB5-Luc with a set of primers (5′-primer, TGTTCGCGAATGTCTGGATCCAAGCTA; 3′-primer, GGTGACTCTAGAGGGTATGGATCCCG) containing the BamHI site and the BamHI-digested fragment was inserted into the BamHI site of pCMV-κB5-Luc. The 10 repeats of the NF-κB binding sequence were amplified from pCMV-κB10-Luc with a set of primers (5′-primer, TGTTCGCGAGTCGACGGATCGGGAGATCT; 3′-primer, ATCTGGCCCGTACATCGCGA) containing NruI sites and the NruI-digested fragment was inserted into the NruI site of pCMV-κB10-Luc to obtain pCMV-κB20-Luc. The sequences of these pDNA preparations were confirmed by automated sequencing. Fig. 1 shows the schematic presentation of these pDNA constructs. Each pDNA was amplified in *E. coli* strain DH5α, then isolated and purified using a Qiagen Endofree™ Plasmid Giga Kit (Qiagen GmbH, Hilden, Germany). The lipopolysaccharide concentration in a pDNA sample was estimated with a LAL assay kit (Limus F Single Test Wako; Wako Pure Chemical, Osaka, Japan) and found to be less than 22 pg/μg DNA. Then, purified pDNA was dissolved in a sterilized endotoxin-free 5% dextrose solution and stored at −20 °C until use.

2.3. In vitro transfection and reporter gene assay

Mouse colon carcinoma colon 26 cells were maintained in RPMI-1640 (Life Technologies Gibco BRL) supplemented with 10% heat-inactivated FBS, penicillin G (100 U/ml) and streptomycin (100 μg/ml) and 4 mM L-glutamine at 37 °C in a 5% CO_2/air humidified atmosphere. Cells were plated on 12-well culture plates at a density of 3×10^5 cells per well

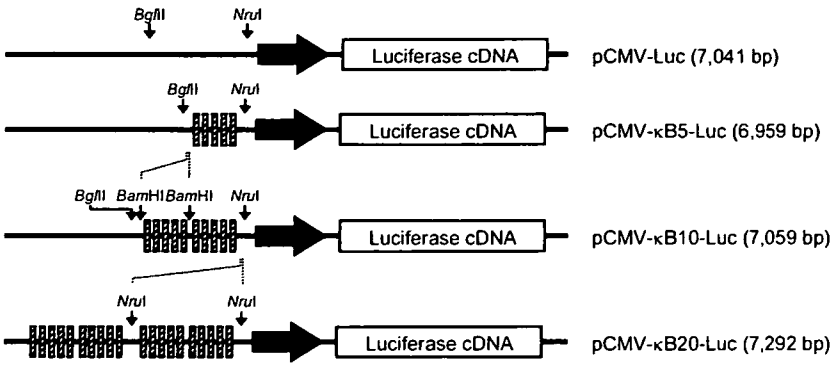

Fig. 1. Schematic presentation of pDNA encoding firefly luciferase cDNA under the control of the human CMV immediate early promoter (black arrow). Each striped box indicates an NF-κB binding sequence (5′-GGGGACTTTCC-3′). The numbers in parentheses indicate the size of each pDNA.

and incubated for 24 h prior to transfection. A pDNA (0.5 μg) encoding firefly luciferase, i.e., pCMV-Luc or pCMV-κB(n)-Luc (n = 5, 10 or 20), and pRL-SV40 (0.1 μg) were complexed with 1.8 μg LipofectAMINE^{TM}2000 (GIBCO-Invitrogen) in 1 ml Opti-MEM. The lipoplex formed was added to the cells and incubated for 4 h. Cells were incubated with PMS (1 or 2 μM) or hydrogen peroxide (100 μM) for 10 h. At 22 h after transfection, the cells were scraped off into a lysis buffer (0.1 M Tris, 0.05% Triton X-100, 2 mM EDTA, pH 7.8), transferred to a 1.5 ml tube and subjected to three cycles of freezing in liquid nitrogen for 3 min and thawing in a water bath at 37 °C for 2 min. The homogenates were centrifuged at 10,000 × g for 8 min at 4 °C. Then, 10 μl of the supernatant was mixed with 100 μl luciferase assay buffer for luciferase assay and then 100 μl of renilla assay buffer was added to the same tube for the renilla assay using the Dual-Luciferase^{TM} Reporter Assay kit (Promega, Madison, WI). The chemiluminescence was measured in a luminometer (Lumat LB 9507, EG&G Berthold, Bad Wildbad, Germany). The luciferase activities were measured and the expression efficiency of pCMV-Luc or pCMV-κB(n)-Luc was evaluated by calculating the ratio of the firefly/renilla luciferase activities. The renilla luciferase was used to normalize any experimental variations among samples, such as transfection efficiency.

2.4. Preparation of nuclear protein extracts

The nuclear protein extracts were collected from colon 26 cells using a nuclear extract kit (Active motif, CA). The concentration of nuclear protein in the supernatant of the extract was determined with the Protein Quantification Kit-Wide range (Dojindo Molecular Technologies Inc., Kumamoto, Japan). To activate NF-κB, colon 26 cells were treated with 4 μM PMS, and the nuclear protein extracts were collected as described above.

2.5. Electrophoretic mobility shift assay (EMSA)

EMSA was performed as described previously (Zhou et al., 1999). The oligonucleotide containing an NF-κB binding sequence and its antisense oligonucleotide were separately end-labeled with [γ-^{32}P]ATP using polynucleotide kinase T4 (MEGALABEL^{TM}, Takara Bio Inc, Otsu, Japan). Both end-labeled oligonucleotides were purified from unincorporated [γ-^{32}P]ATP using a Sephadex G-50 column (Pharmacia, Uppsala, Sweden) and recovered in TNE buffer (10 mM Tris–HCl, 0.1 M NaCl, 1 mM EDTA, pH 7.5). The purified oligonucleotides were incubated for 10 min at room temperature for annealing to obtain the radiolabeled double-stranded DNA probe for EMSA. An aliquot of 60 μg extracted nuclear protein was incubated with a binding buffer (20 mM Hepes, pH 7.9, 0.5 mM EDTA, pH 8.0, 50 mM KCl, 10% glycerol, 0.5 mM DTT, 0.5 mM PMSF) and 2 μg salmon sperm DNA for 15 min on ice. Then, 1.5 × 10^6 cpm of the radiolabeled double-stranded DNA probe was added to the sample followed by an additional 30 min incubation at 4 °C. Two microliters 0.1% bromphenol blue dye was used as a marker. An aliquot of 20 μl of the resulting solution was electrophoresed on a 4% nondenaturing polyacrylamide gel for 90 min at 150 V in TBE buffer in a cold room. After completion of the electrophoresis, the gel was transferred to a piece of blotting paper and dried under vacuum. The dried gel was exposed to an Imaging Plate (Fuji Photo Film, Kanagawa, Japan) and analyzed using a Bio-Image Analyzer System (BAS-2500, Fuji Photo Film). The specificity of the observed signals was also confirmed by using the unlabeled double-strand DNA without any NF-κB binding sequence.

2.6. Statistical analysis

Differences were statistically evaluated by one-way ANOVA followed by the Student-Newmann–Keuls multiple comparison test using SPSS software, and the level of statistical significance was $P < 0.05$.

3. Results

3.1. NF-κB activity in colon carcinoma cells

NF-κB activity was detected by EMSA. The nuclear fractions of colon carcinoma cells were subjected to electrophoresis using ^{32}P-labeled double-stranded oligonucleotides having an NF-κB binding sequence. A band representing the presence of proteins that bind to the DNA probe was detected in the nuclear fraction of colon 26 cells under normal culture conditions (Fig. 2, lane 1), suggesting that NF-κB is constitutively activated in the

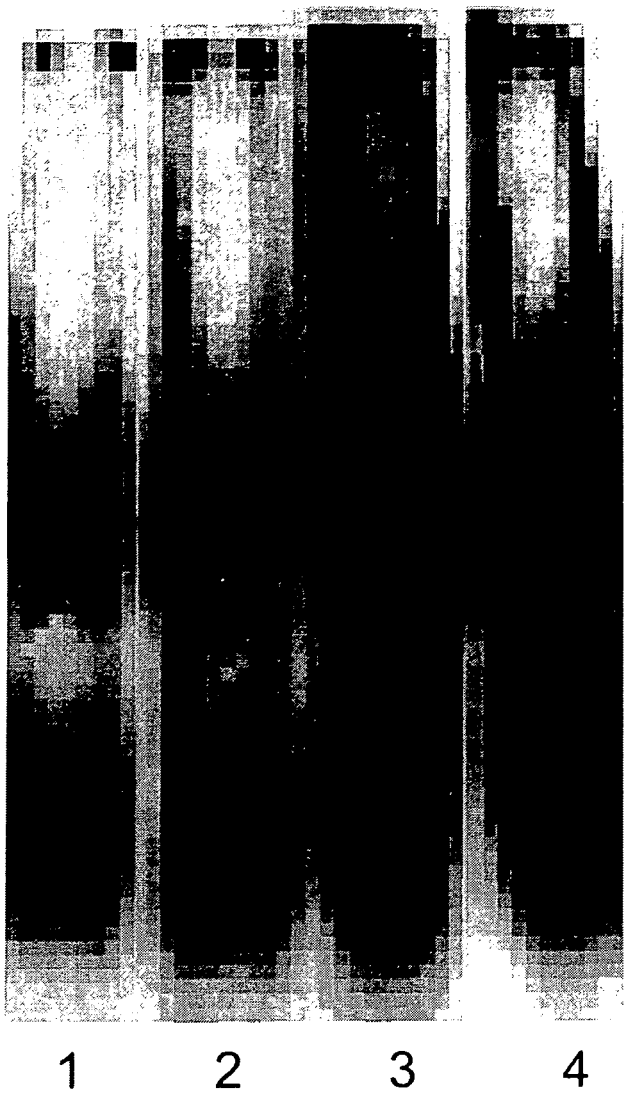

Fig. 2. EMSA analysis of nuclear NF-κB in colon 26 cells. Nuclear proteins extracted from colon 26 cells were analyzed using double-stranded oligonucleotides containing an NF-κB binding sequence (5′-TCAGAGGGGACTTTCCGAGAGG-3′) end-labeled with [γ-^{32}P]ATP. Lane 1, untreated cells. Lanes 2–4, PMS (4 μM), treated cells for 10 h, followed by 0 h (lane 2), 3 h (lane 3), or 10 h (lane 4) incubation in PMS-free medium.

proliferating colon 26 cells. The amount of nuclear NF-κB was increased by PMS treatment (Fig. 2, lane 2). In addition, the activation of NF-κB was also observed at 3 and 10 h after treatment (Fig. 2, lanes 3, and 4, respectively). These results indicate that ROS, which are generated by PMS, activate NF-κB in colon 26 cells, and that the activation lasts for at least 10 h after removal of PMS.

3.2. Increased transgene expression by increasing NF-κB binding sequences in pDNA

Fig. 3 shows the transgene expression in colon 26 cells after transfection of pCMV-Luc, pCMV-κB5-Luc, pCMV-κB10-Luc or pCMV-κB20-Luc. Under control conditions, pCMV-κB5-Luc produced a 1.74-fold increase in transgene expression in colon 26 cells compared with pCMV-Luc ($P < 0.05$). Increasing the number of the NF-κB binding sequences to 10 or 20 further increased the expression ($P < 0.05$ against pCMV-Luc or pCMV-κB5-Luc). A positive correlation between the number of NF-(B binding sequences added and transgene expression was observed ($R^2 = 0.938$). However, the expression almost reached a plateau level when the number of sequence added was 10, and there was no statistically significant difference between the expression levels of pCMV-κB10-Luc and pCMV-κB20-Luc.

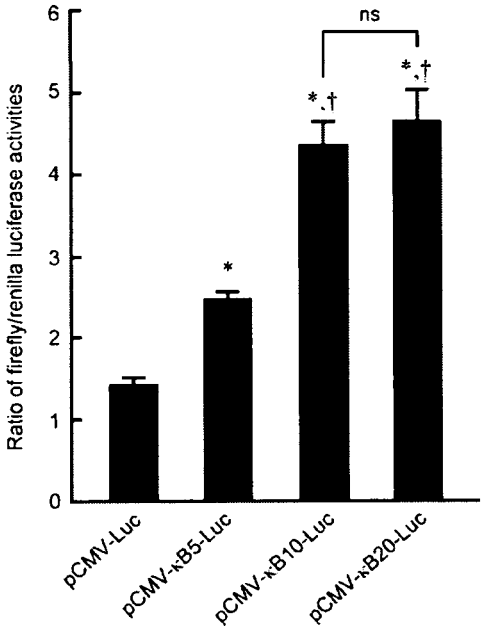

Fig. 3. Transgene expression in colon 26 cells by pCMV-Luc and pCMV-κB(n)-Luc ($n = 5$, 10 or 20). Colon 26 cells were transfected with lipoplex consisting of one of the firefly luciferase-expressing pDNAs (0.5 μg per well) and pRL-SV40 (0.1 μg per well) for 4 h. At 22 h after transfection, firefly and renilla luciferase activities were measured and expressed as the ratio of these activities (mean ± S.D.). *A statistically significant difference ($P < 0.05$) compared with pCMV-Luc; †a statistically significant difference ($P < 0.05$) compared with pCMV-κB5-Luc; ns, not significant.

3.3. Effects of PMS on transgene expression in colon carcinoma cells

Fig. 4A shows the transgene expression by pCMV-Luc or pCMV-κB(n)-Luc in colon 26 cells treated with different concentration of PMS. With any pDNA, the addition of PMS, which generates superoxide anion and hydrogen peroxide, increased the transgene expression in a PMS concentration-dependent manner. Similar results were obtained when the cells were treated with hydrogen peroxide (data not shown). However, under all the conditions examined, pDNA with many NF-κB binding sequences showed higher transgene expression than those with fewer. These results clearly indicate that the novel pDNAs with 10 or 20 NF-κB binding sequences are effective in achieving high transgene expression in cells where NF-κB is highly activated. Linear correlations were observed between the